UNIVERSIDAD DE CONCEPCIÓN

Centro de Investigación en Ingeniería Matemática (CI^{2}MA)

A graph approach for the construction of high order divergence-free Raviart-Thomas finite elements

Ana Alonso-Rodriguez, Jessika Camaño,
Eduardo De Los Santos, Francesca Rapetti

PREPRINT 2018-23

SERIE DE PRE-PUBLICACIONES

A graph approach for the construction of high order divergence-free Raviart-Thomas finite elements

A. Alonso Rodríguez* J. Camaño†‡ E. De Los Santos‡§ F. Rapetti¶

Abstract

We propose and analyze an efficient algorithm for the computation of a basis of the space of divergence-free Raviart-Thomas finite elements. The algorithm is based on graph techniques. The key point is to realize that, with very natural degrees of freedom for fields in the space of Raviart-Thomas finite elements of degree $r+1$ and for elements of the space of discontinuous piecewise polynomial functions of degree $r \geq 0$, the matrix associated with the divergence operator is the incidence matrix of a particular graph. By choosing a spanning tree of this graph, it is possible to identify an invertible square submatrix of the divergence matrix and to compute easily the moments of a field in the space of Raviart-Thomas finite elements with assigned divergence. This approach extends to finite elements of high degree the method introduced by Alotto and Perugia in [4] for finite elements of degree one. The analyzed approach is used to construct a basis of the space of divergence-free Raviart-Thomas finite elements. The numerical tests show that the performance of the algorithm depends neither on the topology of the domain nor or the polynomial degree r.

Keywords: High order Raviart-Thomas finite elements, divergence-free finite elements, spanning tree, oriented graph, incidence matrix.
MSC 2010: 65N30, 05C05 .

1 Introduction

Given a function $\rho \in L^2(\Omega)$, the classical way to compute $\mathbf{u} \in H(\mathrm{div};\Omega)$ such that $\mathrm{div}\,\mathbf{u} = \rho$ is to solve the Dirichlet boundary value problem

$$\begin{cases} \Delta\phi = \rho & \text{in } \Omega\,, \\ \phi = 0 & \text{on } \partial\Omega\,, \end{cases}$$

*Dipartimento di Matematica, Università di Trento, 38123 Povo (Trento), Italy
†Departamento de Matemática y Física Aplicadas, Universidad Católica de la Santísima Concepción
‡CI^{2}MA, Universidad de Concepción, Concepción (Chile)
§Departamento de Ingeniería Matemática, Universidad de Concepción, Chile
¶Dep. de Mathématiques J.-A. Dieudonné, Univ. Côte d'Azur, 06108 Nice cedex 02, France

and take $\mathbf{u} = \operatorname{grad}\phi$. The situation is not so easy if ρ is a discontinuous finite element piecewise polynomial ρ_h and one looks for an approximation $\mathbf{u}_h$ of $\mathbf{u}$ in an appropriate finite element space such that $\operatorname{div}\mathbf{u}_h = \rho_h$. If ρ_h is piecewise constant, then $\mathbf{u}_h$ belongs to the space of Raviart-Thomas finite elements of degree one. For this case an efficient algorithm has been proposed in [3]. We now consider a discrete function ρ_h, that is a polynomial of degree $r \geq 0$ in each tetrahedron of the mesh of Ω, and we look for $\mathbf{u}_h$ in the space of Raviart-Thomas finite elements of degree $r+1$. The algorithm we present is based on graph techniques and extends to higher polynomial degree the ideas introduced in [4] for the case of Raviart-Thomas finite elements of degree one.

The proposed algorithm can be also used to construct a basis of the space of divergence-free Raviart-Thomas finite elements of degree $r+1$. This space appears naturally in different applications. Let us consider the well-known Darcy problem

$$\begin{cases} \mathbf{u} + \mathcal{K}\operatorname{grad} p = \mathbf{g} \ \text{ in } \Omega, \\ \operatorname{div}\mathbf{u} = 0 \ \text{ in } \Omega, \\ \mathbf{u}\cdot\mathbf{n} = 0 \ \text{ on } \partial\Omega, \end{cases}$$

that models the velocity $\mathbf{u}$ of an incompressible fluid flowing in a porous medium occupying the domain Ω, with coefficient of porosity equal to $\mathcal{K}$. Its simpler variational formulation is: find $\mathbf{u} \in H^0(\operatorname{div};\Omega) := \{\mathbf{v} \in H(\operatorname{div};\Omega) \,:\, \operatorname{div}\mathbf{v} = 0\}$ such that

$$\int_\Omega \mathcal{K}^{-1}\mathbf{u}\cdot\mathbf{v} = \int_\Omega \mathcal{K}^{-1}\mathbf{g}\cdot\mathbf{v} \quad \forall\, \mathbf{v} \in H^0(\operatorname{div};\Omega)\,.$$

Let us also mention the electromagnetic problem in its curl-div formulation

$$\begin{cases} \operatorname{curl}\mathbf{u} = \mathbf{J} \ \text{ in } \Omega, \\ \operatorname{div}\mathbf{u} = \rho \ \text{ in } \Omega, \\ \mathbf{u}\times\mathbf{n} = \mathbf{a} \ \text{ or } \ \mathbf{u}\cdot\mathbf{n} = b \ \text{ on } \partial\Omega, \end{cases}$$

as proposed in [1]. For a magnetostatic situation, $\mathbf{u}$ is the magnetic field in Ω generated by an electric current density $\mathbf{J}$ (in this case, $\rho = 0$ and $\mathbf{u}\cdot\mathbf{n} = b$ on $\partial\Omega$). For an electrostatic situation, $\mathbf{u}$ is the electric field in Ω generated by the charge density ρ (in this case, $\mathbf{J} = \mathbf{0}$ and $\mathbf{u}\times\mathbf{n} = \mathbf{a}$ on $\partial\Omega$).

There are different techniques for constructing basis of a divergence free (or approximately divergence free) finite elements spaces in $\mathbb{R}^2$ and $\mathbb{R}^3$; see, for instance, [13], [10], [11], [12], [7], [14], [6]. Concerning the construction of a basis of the space of Raviart-Thomas finite elements that are divergence free, it has been done, for elements of degree one, in [19] for a simply-connected domain with a non-connected boundary (see also [9] where curvilinear elements are considered), in [17] for a g-fold torus, and in [2] for a domain with arbitrary topology. To our knowledge, there are not yet results for the case of Raviart-Thomas finite elements of higher degree. (In [21] the authors

construct a basis of divergence-free finite elements of degree $r \geq 1$ by taking the curl of corresponding potential spaces in two-dimensional domains, $\Omega \subset \mathbb{R}^2$. However in the three-dimensional space this approach is not so direct due to the large kernel of the curl operator.) We treat the three-dimensional case, $\Omega \subset \mathbb{R}^3$, and the same approach is valid in the two-dimensional case too.

This paper is organized as follow. In Section 2 we introduce the necessary notation and briefly present some results of graph theory that will be used in the sequel. Then in Section 3 we write the matrix associated to the divergence operator when using the standard degrees of freedom (moments) for fields in the space of Raviart-Thomas finite elements of degree $r+1$ and for elements of the space of discontinuous piecewise polynomial functions of degree $r \geq 0$. Moreover we prove that it is an incidence matrix of a particular connected graph with no self-loop. Using this last property we compute in Section 4 the moments of a discrete field in the space of Raviart-Thomas finite elements of degree $r+1$ with assigned divergence. Notice that when using high order approximations, the cardinal basis $\{\boldsymbol{\phi}_{h,j}\}_{j=1}^{d_{RT}}$ of the finite elements space with respect to a chosen set of degrees of freedom $\{m_\ell\}_{\ell=1}^{d_{RT}}$, (in this case the moments), has generally to be constructed from a given (favorite) basis $\{\boldsymbol{\psi}_{h,k}\}_{k=1}^{d_{RT}}$ of the finite elements space. This construction involves the inversion of a generalized Vandermonde matrix V, with $[V]_{\ell,k} = m_\ell(\boldsymbol{\psi}_{h,k})$. The inverse matrix V^{-1} provides, column by column, the coefficients to express the cardinal functions as a linear combination of elements of $\{\boldsymbol{\psi}_{h,k}\}_{k=1}^{d_{RT}}$ (see [5]), namely $\boldsymbol{\phi}_{h,j}(\mathbf{x}) = \sum_{k=1}^{d_{RT}} [V^{-1}]_{k,j} \boldsymbol{\psi}_{h,k}(\mathbf{x})$. Once one has the vector $\mathbf{U}$ gathering the moments of a discrete function $\mathbf{u}_h$, and a cardinal basis, we obtain

$$\begin{aligned}\mathbf{u}_h(\mathbf{x}) = \sum_{j=1}^{d_{RT}} U_j \boldsymbol{\phi}_{h,j}(\mathbf{x}) &= \sum_{j=1}^{d_{RT}} U_j \sum_{k=1}^{d_{RT}} [V^{-1}]_{k,j} \boldsymbol{\psi}_{h,k}(\mathbf{x}) \\ &= \sum_{k=1}^{d_{RT}} \sum_{j=1}^{d_{RT}} [V^{-1}]_{k,j} U_j \boldsymbol{\psi}_{h,k}(\mathbf{x}) = \sum_{k=1}^{d_{RT}} \mathbf{U}^\top [V^{-1}]_{k,\cdot} \boldsymbol{\psi}_{h,k}(\mathbf{x})\,.\end{aligned}$$

In Section 5 we use the algorithm presented in Section 4 to compute the moments of a basis of the divergence-free Raviart-Thomas finite elements space for any degree, and Section 6 contains some numerical experiments illustrating the performance of the method for the construction of a basis of the space of divergence-free Raviart-Thomas finite elements of degree two and degree three.

2 Notation and preliminary results

Let Ω be a bounded polyhedral domain of $\mathbb{R}^3$ with Lipschitz boundary. Let us consider a tetrahedral mesh $\mathcal{T}_h = (\mathcal{V}, \mathcal{E}, \mathcal{F}, \mathcal{T})$ over $\overline{\Omega}$. Here $\mathcal{V}$ is the set of vertices, $\mathcal{E}$ that of edges, $\mathcal{F}$ that of faces and $\mathcal{T}$ the set of tetrahedra of $\mathcal{T}_h$. By $n_\mathcal{V}$, $n_\mathcal{E}$, $n_\mathcal{F}$, and $n_\mathcal{T}$ we denote their cardinalities, namely the number of vertices, edges, faces and tetrahedra of the mesh, respectively.

Fixing a total ordering $\mathbf{v}_1, \mathbf{v}_2, \ldots, \mathbf{v}_{n_\mathcal{V}}$ of the elements of $\mathcal{V}$ we induce an orientation of the edges, faces, and tetrahedra of $\mathcal{T}_h$.

- To any edge $e \in \mathcal{E}$ we can associate an increasing function $m_e : \{0,1\} \to \{1,2,\ldots,n_\mathcal{V}\}$ indicating the vertices of e. In this way we assign an (inner) orientation to e and by abuse of notation, the oriented edge $[\mathbf{v}_{m_e(0)}, \mathbf{v}_{m_e(1)}]$ is still denoted by e. The unit tangential vector to e is $\boldsymbol{\tau}_e = \frac{\mathbf{v}_{m_e(1)} - \mathbf{v}_{m_e(0)}}{|\mathbf{v}_{m_e(1)} - \mathbf{v}_{m_e(0)}|}$.
- To any face $f \in \mathcal{F}$ we can associate an increasing function $m_f : \{0,1,2\} \to \{1,2,\ldots,n_\mathcal{V}\}$ indicating the vertices of f. By abuse of notation, the oriented face $[\mathbf{v}_{m_f(0)}, \mathbf{v}_{m_f(1)}, \mathbf{v}_{m_f(2)}]$ is still denoted by f. The unit vector normal to f is $\mathbf{n}_f = \frac{(\mathbf{v}_{m_f(1)} - \mathbf{v}_{m_f(0)}) \times (\mathbf{v}_{m_f(2)} - \mathbf{v}_{m_f(0)})}{|(\mathbf{v}_{m_f(1)} - \mathbf{v}_{m_f(0)}) \times (\mathbf{v}_{m_f(2)} - \mathbf{v}_{m_f(0)})|}$.
- To any tetrahedron $t \in \mathcal{T}$ we can associate an increasing function $m_t : \{0,1,2,3\} \to \{1,2,\ldots,n_\mathcal{V}\}$ indicating the vertices of t. By abuse of notation, the oriented tetrahedron $[\mathbf{v}_{m_t(0)}, \mathbf{v}_{m_t(1)}, \mathbf{v}_{m_t(2)}, \mathbf{v}_{m_t(3)}]$ is still denoted by t. The outward unit vector normal to the boundary ∂t of t is $\mathbf{n}_t$.

We will denote $\Delta_d(\mathcal{T}_h)$ the set of oriented subsimplex of $\mathcal{T}_h$ of dimension $d \leq 3$.

In the following λ_k will be the barycentric coordinate function of the vertex $\mathbf{v}_k$, namely, the continuous piecewise linear function ($\lambda_k|_t \in \mathbb{P}_1$ for all $t \in \mathcal{T}$) such that $\lambda_k(\mathbf{v}_j) = \delta_{k,j}$.

We will use multi-indices of the form

$$\boldsymbol{\eta} \in \mathcal{I}(n, d{+}1) = \left\{ \boldsymbol{\eta}^\top = (\eta_0, \ldots, \eta_d) \in \mathbb{N}^{d+1} : \sum_{i=0}^{d} \eta_i = n \right\}, \ \#\mathcal{I}(n, d{+}1) = \left(\begin{array}{c} n+d \\ d \end{array} \right).$$

For any $\boldsymbol{\eta} \in \mathcal{I}(n, d+1)$ we denote

$$a_{\boldsymbol{\eta}} = \frac{n!}{\eta_0! \eta_1! \cdots \eta_d!}.$$

Given $s \in \Delta_d(\mathcal{T}_h)$ and $\boldsymbol{\eta} \in \mathcal{I}(n, d+1)$ we denote

$$\lambda^{\boldsymbol{\eta}} = \prod_{i=0}^{d} \lambda_{m_s(i)}^{\eta_i}.$$

Note that

$$1 = \left(\sum_{i=0}^{d} \lambda_{m_s(i)}\big|_s \right)^n = \sum_{\boldsymbol{\eta} \in \mathcal{I}(n,d+1)} a_{\boldsymbol{\eta}} \, \lambda^{\boldsymbol{\eta}}. \tag{1}$$

Let $\mathcal{D}_{r+1}$ be the following space of vector polynomials of degree $r+1$ in $\mathbb{R}^3$:

$$\mathcal{D}_{r+1} := (\mathbb{P}_r)^3 \oplus \widetilde{\mathbb{P}}_r \boldsymbol{x}\,,$$

being $\widetilde{\mathbb{P}}_r$ the space of homogeneous polynomials of degree r. The space of Raviart-Thomas finite elements of degree $r+1$ is

$$RT_{h,r+1} = \{\mathbf{z}_h \in H(\mathrm{div};\Omega) \,:\, \mathbf{z}_h|_t \in \mathcal{D}_{r+1}\, \forall\, t \in \mathcal{T}\}\,.$$

It is known that $\dim RT_{h,r+1} = d_{RT} = n_{\mathcal{F}}\binom{r+2}{2} + 3n_{\mathcal{T}}\binom{r-1+3}{3}$. This space have been introduced in [16], but originally it had been introduced in [18] for $\Omega \subset \mathbb{R}^2$.

We denote $P_{h,r}$ the space of discontinuous finite elements that are piecewise polynomial of degree r, namely,

$$P_{h,r} = \{p \in L^2(\Omega) \,:\, p|_t \in \mathbb{P}_r\, \forall\, t \in \mathcal{T}\}\,.$$

It is known that $\dim P_{h,r} = d_P = n_{\mathcal{T}}\binom{r+3}{3}$.

For a brief overview of these spaces and of the Nédélec finite elements of degree $r+1$ that will be mentioned in Section 5, see, e.g., [15]. The classical set of degrees of freedom used to identify the elements of $RT_{h,r+1}$ are moments supported in faces

$$\int_f \mathbf{z}_h \cdot \mathbf{n}_f\, q\,, \quad q \in \mathbb{P}_r(f)\,,\ f \in \mathcal{F}\,,$$

and moments supported in tetrahedra

$$\int_t \mathbf{z}_h \cdot \mathbf{q}\,, \quad \mathbf{q} \in [\mathbb{P}_{r-1}(t)]^3\,,\ t \in \mathcal{T}\,.$$

Similarly, the classical set of degrees of freedom used to identify the elements of $P_{h,r}$ are moments supported in tetrahedra

$$\int_t p_h\, q\,, \quad q \in \mathbb{P}_r(t)\,,\ t \in \mathcal{T}\,.$$

Since we are free to choose any basis of the spaces $\mathbb{P}_r(f)$, $[\mathbb{P}_{r-1}(t)]^3$ and $\mathbb{P}_r(t)$, a possibility is to consider the following set of moments for $RT_{h,r+1}$:

$$C_{\boldsymbol{\alpha}'} \int_f \mathbf{z}_h \cdot \mathbf{n}_f\, \lambda^{\boldsymbol{\alpha}'} \text{ with } \boldsymbol{\alpha}' \in \mathcal{I}(r,3)\,,\ f \in \mathcal{F}\,,$$

and

$$\widehat{C}_{\boldsymbol{\beta}} \int_t \mathbf{z}_h \cdot\ \lambda^{\boldsymbol{\beta}} \operatorname{grad} \lambda_{m_t(j)}\,,\ \text{with } \boldsymbol{\beta} \in \mathcal{I}(r-1,4)\,,\ 1 \le j \le 3\,,\ t \in \mathcal{T}\,.$$

For $P_{h,r}$ one can consider moments of the form

$$C_{\boldsymbol{\alpha}} \int_t p_h \, \lambda^{\boldsymbol{\alpha}} \text{ with } \boldsymbol{\alpha} \in \mathcal{I}(r,4)\,, \;\; t \in \mathcal{T}\,.$$

Here, $C_{\boldsymbol{\alpha}}$, $C_{\boldsymbol{\alpha}'}$ and $\widehat{C}_{\boldsymbol{\beta}}$ are real numbers. We anticipate that we have introduced some parameters in the definition of moments to have the divergence operator represented by an incidence matrix in the high order case, as it occurs naturally in the low order case. We will thus set, for any $\boldsymbol{\eta} \in \mathcal{I}(n, d+1)$,

$$C_{\boldsymbol{\eta}} = a_{\boldsymbol{\eta}} \text{ and } \widehat{C}_{\boldsymbol{\eta}} = (n+1) a_{\boldsymbol{\eta}}\,.$$

We recall some basic definitions and results of graph theory that will be used later (they can be found, for instance, in [20]).

Definition 1. *The all-vertex incidence matrix $M^e \in \mathbb{Z}^{n\times m}$ of a directed graph $\mathcal{M} = (\mathcal{N}, \mathcal{A})$, with n nodes $\mathcal{N} = \{\mathfrak{n}_i\}_{i=1}^n$, m arcs $\mathcal{A} = \{\mathfrak{a}_j\}_{j=1}^m$ and with no self-loop, is the matrix with entries*

$$[M^e]_{i,j} = \begin{cases} 1 & \text{if } \mathfrak{a}_j \text{ is incident on } \mathfrak{n}_i \text{ and oriented away from it,} \\ -1 & \text{if } \mathfrak{a}_j \text{ is incident on } \mathfrak{n}_i \text{ and oriented toward it,} \\ 0 & \text{if } \mathfrak{a}_j \text{ is not incident on } \mathfrak{n}_i\,. \end{cases}$$

An incidence matrix M of $\mathcal{M}$ is any submatrix of M^e with $n-1$ rows and m columns. The node that corresponds to the row of M^e that is not in M will be called the reference node of M.

Note that

$$\operatorname{rank} M^e = \operatorname{rank} M \leq n-1\,,$$

and if $\mathcal{M}$ is connected, then $\operatorname{rank} M^e = \operatorname{rank} M = n-1$, see, e.g., [20, Thm. 6.2].

We recall the definition of spanning tree of a graph $\mathcal{M} = (\mathcal{N}, \mathcal{A})$.

Definition 2. *A tree of a graph $\mathcal{M} = (\mathcal{N}, \mathcal{A})$ is a connected acyclic subgraph of $\mathcal{M}$. A spanning tree $\mathcal{S}$ is a tree of $\mathcal{M}$ containing all its nodes.*

If $\mathcal{S}$ is a spanning tree of $\mathcal{M} = (\mathcal{N}, \mathcal{A})$, then $\mathcal{S} = (\mathcal{N}, \mathcal{B})$ with $\mathcal{B} \subset \mathcal{A}$. Moreover $\mathcal{B}$ has exactly $n-1$ arcs.

In the next sections we will use the following result that joins Theorem 6.9 and Theorem 6.12 in [20].

Theorem 3. *Let $\mathcal{M} = (\mathcal{N}, \mathcal{A})$ be a directed connected graph with no self-loop and $M \in \mathbb{Z}^{(n-1)\times m}$ an incidence matrix of $\mathcal{M}$. Let $\mathcal{S} = (\mathcal{N}, \mathcal{B})$ be a spanning tree of $\mathcal{M}$ and M_{st} the submatrix of order $n-1$ of M given by the columns of M that correspond to the arcs in $\mathcal{B}$. Then M_{st} is invertible and the nonzero elements in each row of M_{st}^{-1} are either all 1 or all -1.*

Proof. The proof can be found, for instance, in [20]. However, for the sake of completeness, we recall in the sequel the main ideas. Each column of M_{st} corresponds to an arc of the spanning tree $\mathcal{S} = (\mathcal{N}, \mathcal{B})$ with $\mathcal{B} = \{\mathfrak{a}_{j(k)}\}_{k=1}^{n-1}$, for a certain function $j : \{1, \ldots, n-1\} \to \{1, \ldots, m\}$.

Each arc $\mathfrak{a}_{j(k)} \in \mathcal{B}$ divides the graph $\mathcal{S}$ in two connected components $\mathcal{S}_r^{(k)}$ and $\mathcal{S}_{nr}^{(k)}$; (the subindex r refers to reference node). We will denote $\mathcal{S}_r^{(k)} = (\mathcal{N}_r^{(k)}, \mathcal{B}_r^{(k)})$ the connected component containing the reference node and $\mathcal{S}_{nr}^{(k)} = (\mathcal{N}_{nr}^{(k)}, \mathcal{B}_{nr}^{(k)})$ the other one. We associate to $\mathfrak{a}_{j(k)}$ the vector $\mathbf{w}^{(k)} \in \mathbb{Z}^{n-1}$ with components:

$$[\mathbf{w}^{(k)}]_i = \begin{cases} -1 & \text{if } \mathfrak{n}_i \notin \mathcal{N}_r^{(k)} \text{ and } \mathfrak{a}_{j(k)} \text{ points from } \mathcal{S}_r^{(k)} \text{ to } \mathcal{S}_{nr}^{(k)}, \\ 1 & \text{if } \mathfrak{n}_i \notin \mathcal{N}_r^{(k)} \text{ and } \mathfrak{a}_{j(k)} \text{ points from } \mathcal{S}_{nr}^{(k)} \text{ to } \mathcal{S}_r^{(k)}, \\ 0 & \text{if } \mathfrak{n}_i \in \mathcal{N}_r^{(k)}. \end{cases}$$

Now we will check that

$$[(\mathbf{w}^{(k)})^\top M_{st}]_l = \delta_{k,l}.$$

In fact, $[(\mathbf{w}^{(k)})^\top M_{st}]_l$ is the scalar product of the vector $\mathbf{w}^{(k)}$ and the column of M_{st} corresponding to the arc $\mathfrak{a}_{j(l)}$.

If the reference node is an extreme node of $\mathfrak{a}_{j(l)}$, then

- for $k \neq l$, the extreme node of $\mathfrak{a}_{j(l)}$ that is not the reference node, is in $\mathcal{N}_r^{(k)}$, hence $[(\mathbf{w}^{(k)})^\top M_{st}]_l = (0)\,(1) = 0$ (if the extreme node, that is not the reference node, is the initial one), or $[(\mathbf{w}^{(k)})^\top M_{st}]_l = (0)\,(-1) = 0$ (if the extreme node, that is not the reference node, is the final one);
- for $k = l$, the extreme node of $\mathfrak{a}_{j(l)}$ that is not the reference node, is not in $\mathcal{N}_r^{(k)}$. If $\mathfrak{a}_{j(k)}$ points from $\mathcal{S}_r^{(k)}$ to $\mathcal{S}_{nr}^{(k)}$, then $[(\mathbf{w}^{(k)})^\top M_{st}]_l = (-1)\,(-1) = 1$ while if $\mathfrak{a}_{j(k)}$ points from $\mathcal{S}_{nr}^{(k)}$ to $\mathcal{S}_r^{(k)}$, then $[(\mathbf{w}^{(k)})^\top M_{st}]_l = (1)\,(1) = 1$.

If the reference node is not an extreme node of $\mathfrak{a}_{j(l)}$, then

- for $k \neq l$, the two extreme nodes of the arc $\mathfrak{a}_{j(l)}$, $\mathfrak{n}_i^l$ and $\mathfrak{n}_{i'}^l$ are in the same connected component $\mathcal{S}_r^{(k)}$ or $\mathcal{S}_{nr}^{(k)}$; we have

$$[(\mathbf{w}^{(k)})^\top M_{st}]_l = \begin{cases} (-1)\,(-1) + (1)\,(-1) & \text{if } \mathfrak{n}_i^l,\, \mathfrak{n}_{i'}^l \notin \mathcal{N}_r^{(k)} \text{ and } \mathfrak{a}_{j(k)} \text{ points from } \mathcal{S}_r^{(k)} \text{ to } \mathcal{S}_{nr}^{(k)} \\ (-1)\,(1) + (1)\,(1) & \text{if } \mathfrak{n}_i^l,\, \mathfrak{n}_{i'}^l \notin \mathcal{N}_r^{(k)} \text{ and } \mathfrak{a}_{j(k)} \text{ points from } \mathcal{S}_{nr}^{(k)} \text{ to } \mathcal{S}_r^{(k)} \\ (-1)\,(0) + (1)\,(0) & \text{if } \mathfrak{n}_i^l,\, \mathfrak{n}_{i'}^l \in \mathcal{N}_r^{(k)} \end{cases}$$

  so $[(\mathbf{w}^{(k)})^\top M_{st}]_l = 0$;
- for $k = l$, one of the extreme nodes of $\mathfrak{a}_{j(l)}$ is in $\mathcal{N}_r^{(k)}$ and the other is not. If $\mathfrak{a}_{j(k)}$ points from $\mathcal{S}_r^{(k)}$ to $\mathcal{S}_{nr}^{(k)}$, then the final node of $\mathfrak{a}_{j(k)}$ (with entry equal -1 in the

k-th column of M_{st}) is not in $\mathcal{N}_r^{(k)}$ and the scalar product is $(-1)(-1)+(0)(1)=1$. If $\mathfrak{a}_{j(k)}$ points from $\mathcal{S}_{nr}^{(k)}$ to $\mathcal{S}_r^{(k)}$, then the initial node of $\mathfrak{a}_{j(k)}$ (with entry equal 1 in the k-th column of M_{st}) is not in $\mathcal{N}_r^{(k)}$ and the scalar product now is $(1)(1)+(0)(-1)=1$.

So, it follows that M_{st}^{-1} is the matrix with entries

$$[M_{st}^{-1}]_{k,j} = [\mathbf{w}^{(k)}]_j\,,$$

since we have showed that

$$\sum_j [M_{st}^{-1}]_{k,j}[M_{st}]_{j,l} = \sum_j [\mathbf{w}^{(k)}]_j [M_{st}]_{j,l} = \delta_{k,l}\,.$$

□

3 The divergence matrix

Our aim now is to identify the matrix that relates the moments of $\mathbf{z}_h \in RT_{h,r+1}$ with the moments of $p_h = \operatorname{div}\mathbf{z}_h \in P_{h,r}$. From the divergence theorem in a tetrahedron, for any $\boldsymbol{\alpha} \in \mathcal{I}(r,4)$ we have

$$\int_t p_h a_{\boldsymbol{\alpha}} \lambda^{\boldsymbol{\alpha}} = \int_t \operatorname{div}\mathbf{z}_h a_{\boldsymbol{\alpha}} \lambda^{\boldsymbol{\alpha}} = \int_{\partial t} \mathbf{z}_h \cdot \mathbf{n}_t\, a_{\boldsymbol{\alpha}} \lambda^{\boldsymbol{\alpha}} - \int_t \mathbf{z}_h \cdot a_{\boldsymbol{\alpha}}\, \operatorname{grad}\lambda^{\boldsymbol{\alpha}}\,. \tag{2}$$

Note that

$$\operatorname{grad}\lambda^{\boldsymbol{\alpha}} = \sum_{i=0}^{d} \alpha_i \lambda^{\boldsymbol{\alpha}-\mathbf{e}_i} \operatorname{grad}\lambda_{m_t(i)}\,,$$

being $\mathbf{e}_i \in \mathbb{N}^4$ the vector with components $(\mathbf{e}_i)_j = \delta_{i,j}$, $0 \le i,j \le 3$. Clearly $\alpha_i \lambda^{\boldsymbol{\alpha}-\mathbf{e}_i}$ is zero if $\alpha_i = 0$, otherwise it is a polynomial of degree $r-1$ of the form $\alpha_i \lambda^{\boldsymbol{\beta}}$ with $\boldsymbol{\beta} \in \mathcal{I}(r-1,4)$. We recall also that, since $1 = \sum_{i=0}^d \lambda_{m_t(i)}$, then $\operatorname{grad}\lambda_{m_t(0)} = -\sum_{i=1}^d \operatorname{grad}\lambda_{m_t(i)}$ on the tetrahedron t. So we have

$$\operatorname{grad}\lambda^{\boldsymbol{\alpha}} = \sum_{i=1}^{d} \left(\alpha_i \lambda^{\boldsymbol{\alpha}-\mathbf{e}_i} - \alpha_0 \lambda^{\boldsymbol{\alpha}-\mathbf{e}_0}\right) \operatorname{grad}\lambda_{m_t(i)}\,.$$

Finally we note that $a_{\boldsymbol{\alpha}}\alpha_i = \frac{r!}{\alpha_0!\cdots\alpha_3!}\alpha_i = r a_{\boldsymbol{\alpha}-\mathbf{e}_i}$, hence

$$\int_t \mathbf{z}_h \cdot a_{\boldsymbol{\alpha}}\, \operatorname{grad}\lambda^{\boldsymbol{\alpha}} = \sum_{i=1}^{d} \int_t \mathbf{z}_h \cdot \left(r a_{\boldsymbol{\alpha}-\mathbf{e}_i} \lambda^{\boldsymbol{\alpha}-\mathbf{e}_i} - r a_{\boldsymbol{\alpha}-\mathbf{e}_0} \lambda^{\boldsymbol{\alpha}-\mathbf{e}_0}\right) \operatorname{grad}\lambda_{m_t(i)}\,.$$

Here $\boldsymbol{\alpha} \in \mathcal{I}(r,4)$. However, if $f \in \partial t$ and $\mathbf{v}_{m_t(i)} \notin f$, then

$$(a_{\boldsymbol{\alpha}}\lambda^{\boldsymbol{\alpha}})|_f = \begin{cases} 0 & \text{if } \alpha_i \neq 0\,, \\ a_{\boldsymbol{\alpha}'}\lambda^{\boldsymbol{\alpha}'} \text{ for a certain } \boldsymbol{\alpha}' \in \mathcal{I}(r,3) & \text{if } \alpha_i = 0\,. \end{cases}$$

The multi-index $\boldsymbol{\alpha}' \in \mathcal{I}(r,3)$ is $R_{t,f}\boldsymbol{\alpha}$, being $R_{t,f} \in \mathbb{Z}^{3\times 4}$ the matrix obtained from the 4×4 identity matrix by omitting the i-th row. For instance, if $f = [\mathbf{v}_{m_t(0)}, \mathbf{v}_{m_t(2)}, \mathbf{v}_{m_t(3)}]$, then

$$\boldsymbol{\alpha}' = R_{t,f}\boldsymbol{\alpha} = \begin{bmatrix} 1 & 0 & 0 & 0 \\ 0 & 0 & 1 & 0 \\ 0 & 0 & 0 & 1 \end{bmatrix} \boldsymbol{\alpha} = \begin{pmatrix} \alpha_0 \\ \alpha_2 \\ \alpha_3 \end{pmatrix}.$$

Notice that, since $\alpha_i = 0$, then $a_{\boldsymbol{\alpha}'} = a_{\boldsymbol{\alpha}}$. Hence

$$\int_{\partial t} \mathbf{z}_h \cdot \mathbf{n}_t \, a_{\boldsymbol{\alpha}} \lambda^{\boldsymbol{\alpha}} = \sum_{f\in\partial t} \mathbf{n}_f \cdot \mathbf{n}_t \int_f \mathbf{z}_h \cdot \mathbf{n}_f \, a_{(R_{t,f}\boldsymbol{\alpha})} \lambda^{(R_{t,f}\boldsymbol{\alpha})},$$

and for each $f \in \partial t$, the multi-index $\boldsymbol{\alpha}' = R_{t,f}\boldsymbol{\alpha}$ is in $\mathcal{I}(r,3)$, as it is the case in moments supported in faces.

So, equation (2) reads

$$\begin{aligned} \int_t \operatorname{div} \mathbf{z}_h a_{\boldsymbol{\alpha}} \lambda^{\boldsymbol{\alpha}} \;=\; & \sum_{f\in\partial t} \mathbf{n}_f \cdot \mathbf{n}_t \int_f \mathbf{z}_h \cdot \mathbf{n}_f \, a_{(R_{t,f}\boldsymbol{\alpha})} \lambda^{(R_{t,f}\boldsymbol{\alpha})} \\ & - \sum_{i=1}^{d} \int_t \mathbf{z}_h \cdot \left(r a_{\boldsymbol{\alpha}-\mathbf{e}_i} \lambda^{\boldsymbol{\alpha}-\mathbf{e}_i} - r a_{\boldsymbol{\alpha}-\mathbf{e}_0} \lambda^{\boldsymbol{\alpha}-\mathbf{e}_0} \right) \operatorname{grad} \lambda_{m_t(i)} \,. \end{aligned} \tag{3}$$

Let $\mathbf{p} \in \mathbb{R}^{d_P}$ be the vector with entries the moments of $p_h = \operatorname{div} \mathbf{z}_h \in P_{h,r}$ and $\mathbf{Z} \in \mathbb{R}^{d_{RT}}$ the vector with entries the moments of $\mathbf{z}_h \in RT_{h,r+1}$, then we can write (3) as:

$$\mathbf{p} = D_{\mathcal{T}_h} \mathbf{Z} \,,$$

where the matrix $D_{\mathcal{T}_h}$ is the matrix associated to the divergence operator that is, in fact, a linear operator from $RT_{h,r+1}$ to $P_{h,r}$.

From the divergence theorem in the whole domain Ω we have also

$$\int_\Omega p_h = \int_\Omega \operatorname{div} \mathbf{z}_h = \int_{\partial\Omega} \mathbf{z}_h \cdot \mathbf{n}_{\partial\Omega} = \sum_{f\in\partial\Omega} \left(\mathbf{n}_f \cdot \mathbf{n}_{\partial\Omega}|_f \int_f \mathbf{z}_h \cdot \mathbf{n}_f \right),$$

where $\mathbf{n}_{\partial\Omega}$ denotes the outward unit vector normal to the boundary $\partial\Omega$. From (1) we have

$$1 = \sum_{\boldsymbol{\alpha}'\in\mathcal{I}(r,3)} a_{\boldsymbol{\alpha}'} \, \lambda^{\boldsymbol{\alpha}'} \Big|_f$$

for any $f \in \mathcal{F}$. Hence

$$-\int_\Omega \operatorname{div} \mathbf{z}_h = -\sum_{f\in\partial\Omega} \left(\mathbf{n}_f \cdot \mathbf{n}_{\partial\Omega}|_f \sum_{\boldsymbol{\alpha}'\in\mathcal{I}(r,3)} \int_f \mathbf{z}_h \cdot \mathbf{n}_f a_{\boldsymbol{\alpha}'} \lambda^{\boldsymbol{\alpha}'} \right). \tag{4}$$

Denoting $\mathbf{p}^e \in \mathbb{R}^{d_P+1}$ the vector $\mathbf{p}^e = [\mathbf{p}^\top, -\int_\Omega p_h]^\top$, we can write (3) and (4) as

$$\mathbf{p}^e = D^e_{\mathcal{T}_h} \mathbf{Z} \,.$$

Proposition 1. *The matrix $D^e_{\mathcal{T}_h}$ is the all-vertex incidence matrix of an oriented graph $\mathcal{M} = (\mathcal{N}, \mathcal{A})$ with $d_P + 1$ nodes: $\binom{r+3}{3}$ for each tetrahedron plus one corresponding to $\partial\Omega$, and d_{RT} arcs. The divergence matrix $D_{\mathcal{T}_h}$ is the incidence matrix with reference node the one corresponding to $\partial\Omega$.*

Proof. To see that each column of $D^e_{\mathcal{T}_h}$ has exactly two elements different from zero, one equal 1 and the other equal -1, we note that each column corresponds to a face moment

$$\int_f \mathbf{z}_h \cdot \mathbf{n}_f \, a_{\boldsymbol{\alpha}'} \lambda^{\boldsymbol{\alpha}'}, \ f \in \mathcal{F}, \ \boldsymbol{\alpha}' \in \mathcal{I}(r,3)\,,$$

or to a tetrahedron moment

$$\int_t \mathbf{z}_h r a_{\boldsymbol{\beta}} \lambda^{\boldsymbol{\beta}} \operatorname{grad} \lambda_{m_t(i)}, \ t \in \mathcal{T}, \ \boldsymbol{\beta} \in \mathcal{I}(r-1,4), \, i = 1,2,3\,.$$

The faces can be internal, if their interior is in Ω, or they can be on the boundary of Ω.

- If f is an internal face, then it belongs to two different tetrahedra, t^- and t^+. Hence, in the column that corresponds to the moment $\int_f \mathbf{z}_h \cdot \mathbf{n}_f a_{\boldsymbol{\alpha}'} \lambda^{\boldsymbol{\alpha}'}$, there are two entries different from zero, one in the row corresponding to the moment $\int_{t^-} p_h a_{(R^\top_{t^-,f}\boldsymbol{\alpha}')} \lambda^{(R^\top_{t^-,f}\boldsymbol{\alpha}')}$ and another one in the row corresponding to the moment $\int_{t^+} p_h a_{(R^\top_{t^+,f}\boldsymbol{\alpha}')} \lambda^{(R^\top_{t^+,f}\boldsymbol{\alpha}')}$. They have opposite sign, because the non zero coefficients are $\mathbf{n}_f \cdot \mathbf{n}_{t^-}$ and $\mathbf{n}_f \cdot \mathbf{n}_{t^+}$, with $\mathbf{n}_{t^-} = -\mathbf{n}_{t^+}$.

- If f is on the boundary of Ω, then it belongs to just one tetrahedron, say $\hat{t}$, and, on f, $\mathbf{n}_{\hat{t}} = \mathbf{n}_{\partial\Omega}$. In the column that corresponds to the moment $\int_f \mathbf{z}_h \cdot \mathbf{n}_f a_{\boldsymbol{\alpha}'} \lambda^{\boldsymbol{\alpha}'}$ there is one entry different from zero in the row corresponding to the moment $\int_{\hat{t}} p_h a_{(R^\top_{\hat{t},f}\boldsymbol{\alpha}')} \lambda^{(R^\top_{\hat{t},f}\boldsymbol{\alpha}')}$. This entry is equal to $\mathbf{n}_f \cdot \mathbf{n}_{\hat{t}}$. There is another entry different from zero in the row corresponding to $\partial\Omega$ with opposite signs, because it is equal to $-(\mathbf{n}_f \cdot \mathbf{n}_{\partial\Omega}) = -(\mathbf{n}_f \cdot \mathbf{n}_{\hat{t}})$.

- The column corresponding to $\int_t \mathbf{z}_h r a_{\boldsymbol{\beta}} \lambda^{\boldsymbol{\beta}} \operatorname{grad} \lambda_{m_t(i)}$ has two entries different from zero: one in the row corresponding to $\int_t p_h a_{\boldsymbol{\beta}+\mathbf{e}_0} \lambda^{\boldsymbol{\beta}+\mathbf{e}_0}$, and the other in the row corresponding to $\int_t p_h a_{\boldsymbol{\beta}+\mathbf{e}_i} \lambda^{\boldsymbol{\beta}+\mathbf{e}_i}$ with opposite sign as can be seen in (3). □

Proposition 2. *The graph $\mathcal{M} = (\mathcal{N}, \mathcal{A})$ corresponding to the all-vertex incidence matrix $D^e_{\mathcal{T}_h}$ is connected.*

Proof. Let us recall that the set of nodes $\mathcal{N}$ is composed by elements of the form

$$\int_t \operatorname{div} \mathbf{z}_h \, a_{\boldsymbol{\alpha}} \lambda^{\boldsymbol{\alpha}}\,, \ t \in \mathcal{T}\,, \ \boldsymbol{\alpha} \in \mathcal{I}(r,4) \qquad \text{and} \qquad \int_{\partial\Omega} \mathbf{z}_h \cdot \mathbf{n}_{\partial\Omega}\,,$$

(that we will denote by $[\boldsymbol{\alpha}, t]$ and $[\partial\Omega]$, respectively) and the set of arcs $\mathcal{A}$, by elements of the form

$$\int_f \mathbf{z}_h \cdot \mathbf{n}_f a_{\boldsymbol{\alpha}'} \lambda^{\boldsymbol{\alpha}'}\,,\ f \in \mathcal{F}\,,\ \boldsymbol{\alpha}' \in \mathcal{I}(r,3)$$

and

$$\int_t \mathbf{z}_h \cdot r a_{\boldsymbol{\beta}} \lambda^{\boldsymbol{\beta}} \operatorname{grad} \lambda_{m_t(i)},\ t \in \mathcal{T},\ \boldsymbol{\beta} \in \mathcal{I}(r-1,4),\ i = 1,2,3,$$

(that we will denote by $[\boldsymbol{\alpha}', f]$, and $[\boldsymbol{\beta}, t, i]$, respectively). As consequence of the divergence theorem, we observe that

(i) for a fixed $t \in \mathcal{T}$ and any $\boldsymbol{\beta} \in \mathcal{I}(r-1,4)$ the arc $[\boldsymbol{\beta}, t, i]$ link the nodes $[\boldsymbol{\beta} + \mathbf{e}_0, t]$ and $[\boldsymbol{\beta} + \mathbf{e}_i, t]$, $i = 1,2,3$.

(ii) for any $\boldsymbol{\alpha}' \in \mathcal{I}(r,3)$, the arc $[\boldsymbol{\alpha}', f]$ link the nodes

$[R^{\top}_{t^-,f}\boldsymbol{\alpha}', t^-]$ and $[R^{\top}_{t^+,f}\boldsymbol{\alpha}', t^+]$, if f is an internal face such that $f = \partial t^+ \cap \partial t^-$ with $t^+, t^- \in \mathcal{T}$.

$[R^{\top}_{t,f}\boldsymbol{\alpha}', t]$ and $[\partial\Omega]$, if f is a face on the boundary of Ω, namely, $f \subseteq \partial t \cap \partial\Omega$ for some $t \in \mathcal{T}$.

Now we will show that, for a fixed $t \in \mathcal{T}$, any two nodes of the set $S(t) = \{[\boldsymbol{\alpha}, t] : \boldsymbol{\alpha} \in \mathcal{I}(r,4)\}$ are connected. More precisely we will show that any node $[\boldsymbol{\alpha}, t] \in S(t)$ is connected with the node $[\overline{\boldsymbol{\alpha}}, t] = [(r,0,0,0), t] \in S(t)$. In fact, by using (i), it is possible to construct a path of length α_1 between the node $[\overline{\boldsymbol{\alpha}}, t]$ and the node $[(r-\alpha_1, \alpha_1, 0, 0), t]$. In the same way, there exists a path of length α_2 between the nodes $[(r-\alpha_1, \alpha_1, 0, 0), t]$ and $[(r-\alpha_1-\alpha_2, \alpha_1, \alpha_2, 0), t]$ and finally, a path of length α_3 between the nodes $[(r-\alpha_1-\alpha_2, \alpha_1, \alpha_2, 0), t]$ and $[(r-\alpha_1-\alpha_2-\alpha_3, \alpha_1, \alpha_2, \alpha_3), t] = [\boldsymbol{\alpha}, t]$. Thus, the nodes $[\overline{\boldsymbol{\alpha}}, t]$ and $[\boldsymbol{\alpha}, t]$ are connected.

Moreover if f is an internal face, then there exists t_1 and t_2 in $\mathcal{T}$ such that $f = \partial t_1 \cap \partial t_2$. From (ii), we know that any arc $[\boldsymbol{\alpha}', f]$ connects the nodes $[R^{\top}_{t_1,f}\boldsymbol{\alpha}', t_1]$ and $[R^{\top}_{t_2,f}\boldsymbol{\alpha}', t_2]$. On the other hand, if f is a face on the boundary of Ω, then $f \subseteq \partial t \cap \partial\Omega$ for some $t \in \mathcal{T}$. In this case, the arc $[\boldsymbol{\alpha}', f]$ connects the nodes $[R^{\top}_{t,f}\boldsymbol{\alpha}', t]$ and $[\partial\Omega]$.

Since Ω is connected we can arrive from any tetrahedron in the mesh to any other following a path constructed by its common faces and this fact guarantees that all nodes are connected. □

Example 1: the case $r = 1$.
The moments of $p_h \in P_{h,1}$ are $\int_t p_h \lambda_{m_t(i)}$ for all $t \in \mathcal{T}$. So, for $0 \le i \le 3$ we have

$$\int_t \operatorname{div} \mathbf{z}_h\ \lambda_{m_t(i)} = \int_{\partial t} \mathbf{z}_h \cdot \mathbf{n}_t\ \lambda_{m_t(i)} - \int_t \mathbf{z}_h \cdot \operatorname{grad} \lambda_{m_t(i)}\,. \tag{5}$$

Moreover

$$\begin{aligned}\partial[\mathbf{v}_{m_t(0)},\mathbf{v}_{m_t(1)},\mathbf{v}_{m_t(2)},\mathbf{v}_{m_t(3)}] &= -[\mathbf{v}_{m_t(0)},\mathbf{v}_{m_t(1)},\mathbf{v}_{m_t(2)}]+[\mathbf{v}_{m_t(0)},\mathbf{v}_{m_t(1)},\mathbf{v}_{m_t(3)}]\\ &\quad -[\mathbf{v}_{m_t(0)},\mathbf{v}_{m_t(2)},\mathbf{v}_{m_t(3)}]+[\mathbf{v}_{m_t(1)},\mathbf{v}_{m_t(2)},\mathbf{v}_{m_t(3)}]\,.\end{aligned}$$

This means that

$$\begin{aligned}\mathbf{n}_t|_{[\mathbf{v}_{m_t(0)},\mathbf{v}_{m_t(1)},\mathbf{v}_{m_t(2)}]} &= -\mathbf{n}_{[\mathbf{v}_{m_t(0)},\mathbf{v}_{m_t(1)},\mathbf{v}_{m_t(2)}]}\,,\\ \mathbf{n}_t|_{[\mathbf{v}_{m_t(0)},\mathbf{v}_{m_t(1)},\mathbf{v}_{m_t(3)}]} &= \mathbf{n}_{[\mathbf{v}_{m_t(0)},\mathbf{v}_{m_t(1)},\mathbf{v}_{m_t(3)}]}\,,\\ \mathbf{n}_t|_{[\mathbf{v}_{m_t(0)},\mathbf{v}_{m_t(2)},\mathbf{v}_{m_t(3)}]} &= -\mathbf{n}_{[\mathbf{v}_{m_t(0)},\mathbf{v}_{m_t(2)},\mathbf{v}_{m_t(3)}]}\,,\\ \mathbf{n}_t|_{[\mathbf{v}_{m_t(1)},\mathbf{v}_{m_t(2)},\mathbf{v}_{m_t(3)}]} &= \mathbf{n}_{[\mathbf{v}_{m_t(1)},\mathbf{v}_{m_t(2)},\mathbf{v}_{m_t(3)}]}\,.\end{aligned}$$

Finally, taking into account that $\operatorname{grad}\lambda_{m_t(0)} = -\sum_{i=1}^{d}\operatorname{grad}\lambda_{m_t(i)}$, we see that the matrix D_t relating the moments of $p_h = \operatorname{div}\mathbf{z}_h \in P_{h,1}$ and $\mathbf{z}_h \in RT_{h,2}$ in a tetrahedron t is

$$D_t = \begin{array}{c}\left[\begin{array}{ccc|ccc|ccc|ccc|ccc}
-1 & 0 & 0 & 1 & 0 & 0 & -1 & 0 & 0 & 0 & 0 & 0 & 1 & 1 & 1\\
0 & -1 & 0 & 0 & 1 & 0 & 0 & 0 & 0 & 1 & 0 & 0 & -1 & 0 & 0\\
0 & 0 & -1 & 0 & 0 & 0 & 0 & -1 & 0 & 0 & 1 & 0 & 0 & -1 & 0\\
0 & 0 & 0 & 0 & 0 & 1 & 0 & 0 & -1 & 0 & 0 & 1 & 0 & 0 & -1
\end{array}\right] \quad [0\,1\,2\,3]\,.\\
\begin{array}{ccccc}[0\,1\,2] & & [0\,1\,3] & & [0\,2\,3] \qquad [1\,2\,3] \qquad [0\,1\,2\,3]\end{array}\end{array}$$

When assembling the whole matrix, $D_{\mathcal{T}_h}$, relating the moments of p_h and $\mathbf{z}_h$, we will have four lines for each tetrahedron, three columns for each face and another three columns for each tetrahedron. In the three columns corresponding to an internal face, there are exactly two non null blocks of four lines corresponding to the two tetrahedra sharing this face. The non zero elements on each block have opposite signs, due to the different orientation of the face on the boundary of the two tetrahedra. On the other hand, each boundary face has exactly one non zero block on its columns, because such a face belongs to the boundary of just one tetrahedron.

Let us consider now the matrix D_t^e that incorporates to D_t a row corresponding to the equation (4)

$$D_t^e = \left[\begin{array}{ccc|ccc|ccc|ccc|ccc}
-1 & 0 & 0 & 1 & 0 & 0 & -1 & 0 & 0 & 0 & 0 & 0 & 1 & 1 & 1\\
0 & -1 & 0 & 0 & 1 & 0 & 0 & 0 & 0 & 1 & 0 & 0 & -1 & 0 & 0\\
0 & 0 & -1 & 0 & 0 & 0 & 0 & -1 & 0 & 0 & 1 & 0 & 0 & -1 & 0\\
0 & 0 & 0 & 0 & 0 & 1 & 0 & 0 & -1 & 0 & 0 & 1 & 0 & 0 & -1\\
1 & 1 & 1 & -1 & -1 & -1 & 1 & 1 & 1 & -1 & -1 & -1 & 0 & 0 & 0
\end{array}\right].$$

The last (blue) row is the one corresponding to equation (4).

Example 2: the case $r = 2$.
The moments of $p_h \in P_{h,2}$ are $\int_t p_h\,(a_{i,j}\lambda_{m_t(i)}\lambda_{m_t(j)})$, for all $t \in \mathcal{T}$, with $0 \le i \le j \le 3$ and

$$a_{i,j} = \begin{cases} 1 & \text{if } i = j\,,\\ 2 & \text{if } i \neq j\,.\end{cases}$$

The face moments in $RT_{h,3}$ are

$$\int_f \mathbf{z}_h \cdot \mathbf{n}_f (a_{i,j} \lambda_{m_f(i)} \lambda_{m_f(j)}) \,, \quad 0 \le i \le j \le 2 \,,$$

and the tetrahedron moments are

$$\int_t \mathbf{z}_h \cdot (2\, \lambda_{m_t(i)} \operatorname{grad} \lambda_{m_t(j)}) \,, \quad 0 \le i \le 3 \,, \quad 1 \le j \le 3 \,.$$

So

$$\int_t \operatorname{div} \mathbf{z}_h \, (a_{i,j} \lambda_{m_t(i)} \lambda_{m_t(j)}) = \int_{\partial t} \mathbf{z}_h \cdot \mathbf{n}_t \, (a_{i,j} \lambda_{m_t(i)} \lambda_{m_t(j)}) - \int_t \mathbf{z}_h \, \operatorname{grad}(a_{i,j} \lambda_{m_t(i)} \lambda_{m_t(j)}) \,,$$

where $\operatorname{grad} \lambda_{m_t(0)} = -\sum_{i=1}^{d} \operatorname{grad} \lambda_{m_t(i)}$ and

$$\operatorname{grad}(a_{i,j} \lambda_{m_t(i)} \lambda_{m_t(j)}) = a_{i,j} (\lambda_{m_t(i)} \operatorname{grad} \lambda_{m_t(j)} + \lambda_{m_t(j)} \operatorname{grad} \lambda_{m_t(i)}) =$$

$$= \begin{cases} 2 \lambda_{m_t(i)} \operatorname{grad} \lambda_{m_t(i)} & \text{if } i = j \,, \\ 2 (\lambda_{m_t(i)} \operatorname{grad} \lambda_{m_t(j)} + \lambda_{m_t(j)} \operatorname{grad} \lambda_{m_t(i)}) & \text{if } i \ne j \,. \end{cases}$$

So in the case of just one tetrahedron we can write the divergence matrix. We divide it in two blocks: the block D^{tf}, that relates the tetrahedron moments of $P_{h,2}$ with the face moments of $RT_{h,3}$, and the block D^{tt}, that relates the tetrahedron moments of $P_{h,2}$ with the tetrahedron moments of $RT_{h,3}$.

$$\begin{array}{c} \\ 00 \\ 01 \\ 02 \\ 03 \\ 11 \\ 12 \\ 13 \\ 22 \\ 23 \\ 33 \end{array} \left[\begin{array}{cccccc|cccccc|cccccc|cccccc} -1 & 0 & 0 & 0 & 0 & 0 & 1 & 0 & 0 & 0 & 0 & 0 & -1 & 0 & 0 & 0 & 0 & 0 & 0 & 0 & 0 & 0 & 0 & 0 \\ 0 & -1 & 0 & 0 & 0 & 0 & 0 & 1 & 0 & 0 & 0 & 0 & 0 & 0 & 0 & 0 & 0 & 0 & 0 & 0 & 0 & 0 & 0 & 0 \\ 0 & 0 & -1 & 0 & 0 & 0 & 0 & 0 & 0 & 0 & 0 & 0 & 0 & -1 & 0 & 0 & 0 & 0 & 0 & 0 & 0 & 0 & 0 & 0 \\ 0 & 0 & 0 & 0 & 0 & 0 & 0 & 0 & 1 & 0 & 0 & 0 & 0 & 0 & -1 & 0 & 0 & 0 & 0 & 0 & 0 & 0 & 0 & 0 \\ 0 & 0 & 0 & -1 & 0 & 0 & 0 & 0 & 0 & 1 & 0 & 0 & 0 & 0 & 0 & 0 & 0 & 0 & 1 & 0 & 0 & 0 & 0 & 0 \\ 0 & 0 & 0 & 0 & -1 & 0 & 0 & 0 & 0 & 0 & 0 & 0 & 0 & 0 & 0 & 0 & 0 & 0 & 0 & 1 & 0 & 0 & 0 & 0 \\ 0 & 0 & 0 & 0 & 0 & 0 & 0 & 0 & 0 & 0 & 1 & 0 & 0 & 0 & 0 & 0 & 0 & 0 & 0 & 0 & 1 & 0 & 0 & 0 \\ 0 & 0 & 0 & 0 & 0 & -1 & 0 & 0 & 0 & 0 & 0 & 0 & 0 & 0 & 0 & -1 & 0 & 0 & 0 & 0 & 0 & 1 & 0 & 0 \\ 0 & 0 & 0 & 0 & 0 & 0 & 0 & 0 & 0 & 0 & 0 & 0 & 0 & 0 & 0 & 0 & -1 & 0 & 0 & 0 & 0 & 0 & 1 & 0 \\ 0 & 0 & 0 & 0 & 0 & 0 & 0 & 0 & 0 & 0 & 0 & 1 & 0 & 0 & 0 & 0 & 0 & -1 & 0 & 0 & 0 & 0 & 0 & 1 \end{array} \right] = D^{tf} \,,$$

$$\begin{array}{c} 00\ 01\ 02\ 11\ 12\ 22 \\ [0\,1\,2] \end{array} \quad \begin{array}{c} 00\ 01\ 03\ 11\ 13\ 33 \\ [0\,1\,3] \end{array} \quad \begin{array}{c} 00\ 02\ 03\ 22\ 23\ 33 \\ [0\,2\,3] \end{array} \quad \begin{array}{c} 11\ 12\ 13\ 22\ 23\ 33 \\ [1\,2\,3] \end{array}$$

$$\begin{array}{c} \\ 00 \\ 01 \\ 02 \\ 03 \\ 11 \\ 12 \\ 13 \\ 22 \\ 23 \\ 33 \end{array} \left[\begin{array}{cccccccccccccc} 1 & 1 & 1 & 0 & 0 & 0 & 0 & 0 & 0 & 0 & 0 & 0 & 0 & 0 \\ -1 & 0 & 0 & 1 & 1 & 1 & 0 & 0 & 0 & 0 & 0 & 0 & 0 & 0 \\ 0 & -1 & 0 & 0 & 0 & 0 & 1 & 1 & 1 & 0 & 0 & 0 & 0 & 0 \\ 0 & 0 & -1 & 0 & 0 & 0 & 0 & 0 & 0 & 1 & 1 & 1 & 1 & 1 \\ 0 & 0 & 0 & -1 & 0 & 0 & 0 & 0 & 0 & 0 & 0 & 0 & 0 & 0 \\ 0 & 0 & 0 & 0 & -1 & 0 & -1 & 0 & 0 & 0 & 0 & 0 & 0 & 0 \\ 0 & 0 & 0 & 0 & 0 & -1 & 0 & 0 & 0 & -1 & 0 & 0 & 0 & 0 \\ 0 & 0 & 0 & 0 & 0 & 0 & 0 & -1 & 0 & 0 & 0 & 0 & 0 & 0 \\ 0 & 0 & 0 & 0 & 0 & 0 & 0 & 0 & -1 & 0 & -1 & 0 & 0 & 0 \\ 0 & 0 & 0 & 0 & 0 & 0 & 0 & 0 & 0 & 0 & 0 & 0 & -1 & 0 \end{array} \right] = D^{tt} \,.$$

$$01\ \ 02\ \ 03\ \ 11\ \ 12\ \ 13\ \ 21\ \ 22\ \ 23\ \ 31\ \ 32\ \ 33$$

Then

$$D_t = [D^{tf}\,, D^{tt}]\,.$$

4 An element of $RT_{h,r+1}$ with assigned divergence

We now propose an efficient algorithm for the computation of the moments of a solution of the following problem: given $\rho_h \in P_{h,r}$, find $\mathbf{u}_h \in RT_{h,r+1}$ such that $\operatorname{div} \mathbf{u}_h = \rho_h$. Denoting $\mathbf{U} \in \mathbb{R}^{d_{RT}}$ the vector with entries the moments of $\mathbf{u}_h$ and $\boldsymbol{\rho} \in \mathbb{R}^{d_P}$ the vector with entries the moments of ρ_h, we are looking for a solution of the rectangular linear system

$$D_{\mathcal{T}_h}\mathbf{U} = \boldsymbol{\rho}\,. \tag{6}$$

Let $\mathcal{S} = (\mathcal{N}, \mathcal{B})$ be a spanning tree of $\mathcal{M} = (\mathcal{N}, \mathcal{A})$. By definition $\mathcal{B}$ has exactly d_P of the d_{RT} arcs of $\mathcal{A}$. For instance, if $r = 1$, the submatrix in red of the matrix D_t^e below

$$D_t^e = \left[\begin{array}{rrrrrrrrrrrrrrr}
-1 & 0 & 0 & 1 & 0 & 0 & -1 & 0 & 0 & 0 & 0 & 0 & 1 & 1 & 1 \\
0 & -1 & 0 & 0 & 1 & 0 & 0 & 0 & 0 & 1 & 0 & 0 & -1 & 0 & 0 \\
0 & 0 & -1 & 0 & 0 & 0 & 0 & -1 & 0 & 0 & 1 & 0 & 0 & -1 & 0 \\
0 & 0 & 0 & 0 & 0 & 1 & 0 & 0 & -1 & 0 & 0 & 1 & 0 & 0 & -1 \\
1 & 1 & 1 & -1 & -1 & -1 & 1 & 1 & 1 & -1 & -1 & -1 & 0 & 0 & 0
\end{array}\right],$$

is the all-vertex incidence matrix of a spanning tree $\mathcal{S}$ of $\mathcal{M}$. In Figure 1 we present, on the left, the graph $\mathcal{M}$ (one style of line for each block of three columns in the matrix D_t^e), and on the right, the spanning tree $\mathcal{S}$.

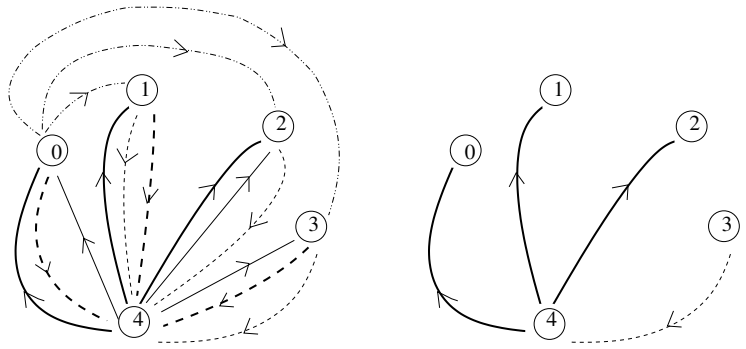

Figure 1: The graph $\mathcal{M}$ that corresponds to the matrix D_t^e with a different style of line for each three-column block in D_t^e (left) and the spanning tree $\mathcal{S}$ (right).

In the matrix $D_{\mathcal{T}_h}$ we distinguish the columns corresponding to the arcs in $\mathcal{S}$ (and we denote D_{st} the submatrix of $D_{\mathcal{T}_h}$ composed by these columns; the subindex st refers to spanning tree), and the columns corresponding to arcs not in $\mathcal{S}$ (and we denote D_{ct}

the submatrix of $D_{\mathcal{T}_h}$ composed by these columns; the subindex *ct* refers to co-tree). So, reordering the columns of $D_{\mathcal{T}_h}$ by using a permutation matrix P, we can write

$$D_{\mathcal{T}_h} P = [D_{st}, D_{ct}] .$$

From Theorem 3 and Propositions 1 and 2, we know that D_{st} is non singular. Denoting $\mathfrak{U} = P^\top \mathbf{U}$, we have

$$D_{\mathcal{T}_h} \mathbf{U} = \boldsymbol{\rho} \Leftrightarrow D_{\mathcal{T}_h} P \mathfrak{U} = \boldsymbol{\rho} ,$$

and $D_{\mathcal{T}_h} P = [D_{st},\, D_{ct}]$. So, if we denote $\mathfrak{U}_{st}$ the vector with the first d_P components of $\mathfrak{U}$ and $\mathfrak{U}_{ct}$ the vector with the remaining $d_{RT} - d_P$ components, we can write the rectangular linear system to be solved as

$$D_{st}\, \mathfrak{U}_{st} + D_{ct}\, \mathfrak{U}_{ct} = \boldsymbol{\rho} . \tag{7}$$

For any choice of $\mathfrak{U}_{ct} \in \mathbb{R}^{d_{RT}-d_P}$, solving $D_{st}\mathfrak{U}_{st} = \boldsymbol{\rho} - D_{ct}\mathfrak{U}_{ct}$, we obtain a solution of (7). If we choose for instance $\mathfrak{U}_{ct} = \mathbf{0}$ we obtain

$$\mathfrak{U} = \begin{bmatrix} D_{st}^{-1}\boldsymbol{\rho} \\ \mathbf{0} \end{bmatrix} ,$$

and then $\mathbf{U} = P\mathfrak{U}$.

5 A basis of the space $RT^0_{h,r+1} = RT_{h,r+1} \cap H^0(\mathrm{div};\Omega)$

Proceeding in a similar way, we can compute the moments of the elements of a basis of the space $RT^0_{h,r+1} = RT_{h,r+1} \cap H^0(\mathrm{div};\Omega)$.

Proposition 3. *The columns of the matrix*

$$B = P \begin{bmatrix} -D_{st}^{-1} D_{ct} \\ I \end{bmatrix} \in \mathbb{Z}^{d_{RT} \times (d_{RT}-d_P)} ,$$

being I the identity matrix in $\mathbb{R}^{(d_{RT}-d_P)\times(d_{RT}-d_P)}$, are the moments of $d_{RT} - d_P$ linear independent functions in $RT_{h,r+1}$, that are divergence-free.

Proof. Taking $\boldsymbol{\rho} = \mathbf{0}$ in (7) and replacing $\mathfrak{U}_{ct}$ with the identity matrix of dimension $d_{RT} - d_P$, it is easy to check that

$$D_{\mathcal{T}_h} B = D_{\mathcal{T}_h} P \begin{bmatrix} -D_{st}^{-1} D_{ct} \\ I \end{bmatrix} = [D_{st}\, , D_{ct}] \begin{bmatrix} -D_{st}^{-1} D_{ct} \\ I \end{bmatrix} = -D_{ct} + D_{ct} = 0 .$$

The fact that the corresponding functions are linearly independent is a consequence of the identity block in the definition of B. □

Let $N_{h,r+1}$ be the space of Nédélec curl conforming finite elements of degree $r+1$. If $\partial\Omega$ has $p+1$ connected components $(\partial\Omega)_0,\ldots,(\partial\Omega)_p$, then it is well known (see e.g. [8]) that given $\mathbf{z}_h \in RT_{h,r+1}$, there exists $\mathbf{w}_h \in N_{h,r+1}$, such that $\operatorname{curl}\mathbf{w}_h = \mathbf{z}_h$ if and only if $\operatorname{div}\mathbf{z}_h = 0$ and $\int_{(\partial\Omega)_k} \mathbf{z}_h\cdot\mathbf{n}_{\partial\Omega} = 0$, for $k = 1,2,\ldots,p$. Moreover, the dimension of the space of functions in $H^0(\operatorname{div};\Omega)$ that are not the curl of any vector potential in $H(\operatorname{curl};\Omega)$ (the second de Rham cohomology group) is equal to p.

It is possible to construct a basis of the space $RT^0_{h,r+1}$ with p elements that are representatives of a basis of the second de Rham cohomology group and the remaining $d_{RT}-(p+d_P)$ that are the curl of vector potentials in $N_{h,r+1}$.

Let $(\partial\Omega)_0$ be the external connected component of $\partial\Omega$. We consider the following problem: given $\rho_h \in P_{h,r}$ and $\mathbf{C}\in\mathbb{R}^p$, find $\widetilde{\mathbf{u}}_h \in RT_{h,r+1}$ such that

$$\begin{cases} \operatorname{div}\widetilde{\mathbf{u}}_h = \rho_h\,, \\ \int_{(\partial\Omega)_k}\widetilde{\mathbf{u}}_h\cdot\mathbf{n}_{\partial\Omega} = C_k\,, \quad \text{for } k=1,2,\ldots,p\,. \end{cases}$$

The number of equations is now equal to d_P+p, while the number of unknowns remains equal to d_{RT}. From (1), we have $1 = \sum_{\boldsymbol{\alpha}'\in\mathcal{I}(r,3)} a_{\boldsymbol{\alpha}'}\,\lambda^{\boldsymbol{\alpha}'}\Big|_f$ for any $f\in\mathcal{F}$, hence

$$\begin{aligned} \int_{(\partial\Omega)_k}\widetilde{\mathbf{u}}_h\cdot\mathbf{n}_{\partial\Omega} &= \sum_{f\in(\partial\Omega)_k}\left(\mathbf{n}_f\cdot\mathbf{n}_{\partial\Omega}|_f\int_f\widetilde{\mathbf{u}}_h\cdot\mathbf{n}_f\right) \\ &= \sum_{f\in(\partial\Omega)_k}\left(\mathbf{n}_f\cdot\mathbf{n}_{\partial\Omega}|_f\sum_{\boldsymbol{\alpha}'\in\mathcal{I}(r,3)}\int_f\widetilde{\mathbf{u}}_h\cdot\mathbf{n}_f a_{\boldsymbol{\alpha}'}\lambda^{\boldsymbol{\alpha}'}\right). \end{aligned}$$

So, the new p equations (multiplied by -1) can be written as

$$-\sum_{f\in(\partial\Omega)_k}\left(\mathbf{n}_f\cdot\mathbf{n}_{\partial\Omega}|_f\sum_{\boldsymbol{\alpha}'\in\mathcal{I}(r,3)}\int_f\widetilde{\mathbf{u}}_h\cdot\mathbf{n}_f a_{\boldsymbol{\alpha}'}\lambda^{\boldsymbol{\alpha}'}\right) = -C_k,\quad k=1,\ldots,p\,, \tag{8}$$

or using matrix notation, $H\widetilde{\mathbf{U}} = -\mathbf{C}$, being $\widetilde{\mathbf{U}}\in\mathbb{R}^{d_{RT}}$ the vector with the moments of $\widetilde{\mathbf{u}}_h$. Note that the entries of matrix $H\in\mathbb{R}^{p\times d_{RT}}$ are 0, if $f\notin(\partial\Omega)_k$, or, $-\mathbf{n}_f\cdot\mathbf{n}_{\partial\Omega}|_f$, that is equal to 1 or -1, if $f\in(\partial\Omega)_k$.

Denoting by $\mathbf{V}\in\mathbb{R}^{d_P+p}$ the vector $\mathbf{V} = \begin{bmatrix}\boldsymbol{\rho}\\ \mathbf{C}\end{bmatrix}$ and by $\widetilde{D}_{\mathcal{T}_h}\in\mathbb{R}^{(d_P+p)\times d_{RT}}$ the matrix $\widetilde{D}_{\mathcal{T}_h} = \begin{bmatrix} D_{\mathcal{T}_h}\\ H\end{bmatrix}$, we want to solve the rectangular linear system $\widetilde{D}_{\mathcal{T}_h}\widetilde{\mathbf{U}} = \mathbf{V}$.

The matrix $\widetilde{D}_{\mathcal{T}_h}\in\mathbb{R}^{(d_P+p)\times d_{RT}}$ is an incidence matrix of a new connected and directed graph $\widetilde{\mathcal{M}} = (\widetilde{\mathcal{N}},\widetilde{\mathcal{A}})$, with no self loops. This new graph $\widetilde{\mathcal{M}}$ is similar to the graph $\mathcal{M}$: the node of $\mathcal{M}$ that corresponds to $\partial\Omega$ has been replaced in $\widetilde{\mathcal{M}}$ by $p+1$ nodes corresponding to the different connected components of $\partial\Omega$

$$\int_{(\partial\Omega)_k}\mathbf{z}_h\cdot\mathbf{n}_{\partial\Omega}\,,\ k=0,...,p\,,$$

and the number of arcs in $\widetilde{\mathcal{M}}$ is equal to the number of arcs in $\mathcal{M}$. If f is a face on $\partial\Omega$, then $f \subseteq (\partial\Omega)_k \cap \partial t$ for some $t \in \mathcal{T}$ and some $k \in \{0, ..., p\}$. In this case the arc $[\boldsymbol{\alpha}', f]$, with $\boldsymbol{\alpha}' \in \mathcal{I}(r, 3)$, connects the nodes $[R_{t,f}^{\top}\boldsymbol{\alpha}', t]$ and $[(\partial\Omega)_k]$ of the graph $\widetilde{\mathcal{M}}$ and hence also $\widetilde{\mathcal{M}}$ is connected.

The all-vertex incidence matrix of $\widetilde{\mathcal{M}} = (\widetilde{\mathcal{N}}, \widetilde{\mathcal{A}})$ has a row for each connected component of $\partial\Omega$. The sum of these $p+1$ rows is equal to the row corresponding to $\partial\Omega$ in the all-vertex incidence matrix of $\mathcal{M}$. The reference node for the incidence matrix $\widetilde{D}_{\mathcal{T}_h}$ is the one that corresponds to the external connected component of $\partial\Omega$, $(\partial\Omega)_0$. This means that in the matrix $\widetilde{D}_{\mathcal{T}_h}$ all the columns corresponding to tetrahedron moments or face moments for internal faces have exactly two entries different from zero, one equal to 1 and the other equal to -1. Both of them are in rows of $D_{\mathcal{T}_h}$. But in $\widetilde{D}_{\mathcal{T}_h}$ also the columns that correspond to face moments for a face $f \in (\partial\Omega)_k$ with $k \in \{1, \ldots, p\}$ have two entries different from zero, one in $D_{\mathcal{T}_h}$ and the other in the k-th row of H. Only the columns that correspond to face moments for a face $f \in (\partial\Omega)_0$ have just one entry different from zero.

Let $\widetilde{\mathcal{S}}$ be a spanning tree of $\widetilde{\mathcal{M}}$. According to $\widetilde{\mathcal{S}}$ we identify a set of $d_P + p$ columns of $\widetilde{D}_{\mathcal{T}_h}$ that compose an invertible matrix $\widetilde{D}_{st}$. Reordering the columns of $\widetilde{D}_{\mathcal{T}_h}$ we can write $\widetilde{D}_{\mathcal{T}_h}\widetilde{P} = [\widetilde{D}_{st}\,, \widetilde{D}_{ct}]$. Now we have $\widetilde{D}_{st} \in \mathbb{Z}^{(d_P+p)\times(d_P+p)}$ and $\widetilde{D}_{ct} \in \mathbb{Z}^{(d_P+p)\times(d_{RT}-(d_P+p))}$.

Proceeding as before and denoting $\widetilde{\mathfrak{U}} = \widetilde{P}^{\top}\widetilde{\mathbf{U}}$ we can write

$$\widetilde{D}_{\mathcal{T}_h}\widetilde{\mathbf{U}} = \mathbf{V} \Leftrightarrow \widetilde{D}_{\mathcal{T}_h}\widetilde{P}\widetilde{\mathfrak{U}} = \mathbf{V} \Leftrightarrow [\widetilde{D}_{st}\,, \widetilde{D}_{ct}] \begin{bmatrix} \widetilde{\mathfrak{U}}_{st} \\ \widetilde{\mathfrak{U}}_{ct} \end{bmatrix} = \mathbf{V}\,.$$

Here $\widetilde{\mathfrak{U}}_{st}$ is the vector with the first $d_P + p$ components of $\widetilde{\mathfrak{U}}$ and $\widetilde{\mathfrak{U}}_{ct}$ the vector with the remaining $d_{RT} - (d_P + p)$ components. Hence

$$\widetilde{D}_{st}\widetilde{\mathfrak{U}}_{st} = \mathbf{V} - \widetilde{D}_{ct}\widetilde{\mathfrak{U}}_{ct} = \begin{bmatrix} \boldsymbol{\rho} \\ \mathbf{C} \end{bmatrix} - \widetilde{D}_{ct}\widetilde{\mathfrak{U}}_{ct}\,.$$

Let $\widehat{\mathbf{e}}_k$, $k \in \{1, \ldots, p\}$ be the elements of the canonical basis of $\mathbb{R}^p$ and let $\mathbf{e}_j$, $j \in \{1, \ldots, d_{RT} - (p + d_P)\}$ be the elements of the canonical basis of $\mathbb{R}^{d_{RT}-(d_P+p)}$. Let us consider $\boldsymbol{\rho} = \mathbf{0}$. For $k \in \{1, \ldots, p\}$, we denote $\widetilde{\mathfrak{U}}_{st,k} \in \mathbb{Z}^{d_P+p}$ the solution of the linear system

$$\widetilde{D}_{st}\widetilde{\mathfrak{U}}_{st,k} = \begin{bmatrix} \mathbf{0} \\ \widehat{\mathbf{e}}_k \end{bmatrix},$$

and for $j \in \{1, \ldots, d_{RT} - (p + d_P)\}$, we denote $\widetilde{\mathfrak{U}}_{st,p+j} \in \mathbb{Z}^{d_P+p}$ the solution of the linear system

$$\widetilde{D}_{st}\widetilde{\mathfrak{U}}_{st,p+j} = -\widetilde{D}_{ct}\mathbf{e}_j\,.$$

We denote, respectively, $N_1 \in \mathbb{R}^{(d_P+p)\times p}$ the matrix with column k equal to $\widetilde{\mathfrak{U}}_{st,k}$, and $N_2 \in \mathbb{R}^{(d_P+p)\times(d_{RT}-(d_P+p))}$ the matrix with column j equal to $\widetilde{\mathfrak{U}}_{st,p+j}$. It follows that

$$\widetilde{D}_{st}N_1 = \begin{bmatrix} 0 \\ I_p \end{bmatrix} =: \widetilde{I} \quad \text{and} \quad \widetilde{D}_{st}N_2 = -\widetilde{D}_{ct}\,,$$

being I_p the identity matrix in $\mathbb{R}^{p\times p}$. In a more compact way we have

$$\widetilde{D}_{st}N = [\widetilde{I}, -\widetilde{D}_{ct}]\,, \tag{9}$$

with $\widetilde{D}_{st} \in \mathbb{Z}^{(d_P+p)\times(d_P+p)}$, $N = [N_1, N_2] \in \mathbb{R}^{(d_P+p)\times(d_{RT}-d_P)}$, $\widetilde{I} \in \mathbb{R}^{(d_P+p)\times p}$ and $-\widetilde{D}_{ct} \in \mathbb{Z}^{(d_P+p)\times(d_{RT}-(d_P+p))}$.

Proposition 4. *The columns of the matrix*

$$\widetilde{B}_1 = \widetilde{P}\begin{bmatrix} N_1 \\ 0 \end{bmatrix} \in \mathbb{Z}^{d_{RT}\times p}$$

are the moments of functions $\widetilde{\mathbf{u}}_{h,k} \in RT_{h,r+1}$ such that

$$\begin{cases} \operatorname{div}\widetilde{\mathbf{u}}_{h,k} = 0\,, \\ \int_{(\partial\Omega)_l} \widetilde{\mathbf{u}}_{h,k}\cdot\mathbf{n}_{\partial\Omega} = \delta_{k,l} \quad \textit{for } l = 1,2,\dots,p\,. \end{cases}$$

The columns of the matrix

$$\widetilde{B}_2 = \widetilde{P}\begin{bmatrix} N_2 \\ I_{d_{RT}-(d_P+p)} \end{bmatrix} \in \mathbb{Z}^{d_{RT}\times(d_{RT}-(d_P+p))}\,,$$

being $I_{d_{RT}-(d_P+p)}$ the identity matrix in $\mathbb{R}^{(d_{RT}-(d_P+p))\times(d_{RT}-(d_P+p))}$, are the moments of $d_{RT}-(d_P+p)$ linearly independent functions, $\widetilde{\mathbf{u}}_{h,p+j} \in RT_{h,r+1}$, such that

$$\begin{cases} \operatorname{div}\widetilde{\mathbf{u}}_{h,p+j} = 0\,, \\ \int_{(\partial\Omega)_l} \widetilde{\mathbf{u}}_{h,p+j}\cdot\mathbf{n}_{\partial\Omega} = 0 \quad \textit{for } l = 1,2,\dots,p\,. \end{cases}$$

Proof. It is enough to check that $\widetilde{D}_{\mathcal{T}_h}\widetilde{B}_1 = \begin{bmatrix} 0 \\ I_p \end{bmatrix}$ and $\widetilde{D}_{\mathcal{T}_h}\widetilde{B}_2 = 0$. In fact,

$$\widetilde{D}_{\mathcal{T}_h}\widetilde{B}_1 = \widetilde{D}_{\mathcal{T}_h}\widetilde{P}\begin{bmatrix} N_1 \\ 0 \end{bmatrix} = [\widetilde{D}_{st}\,, \widetilde{D}_{ct}]\begin{bmatrix} N_1 \\ 0 \end{bmatrix} = \widetilde{D}_{st}N_1 = \begin{bmatrix} 0 \\ I_p \end{bmatrix}.$$

On the other hand

$$\widetilde{D}_{\mathcal{T}_h}\widetilde{B}_2 = \widetilde{D}_{\mathcal{T}_h}\widetilde{P}\begin{bmatrix} N_2 \\ I_{d_{RT}-(d_P+p)} \end{bmatrix} = [\widetilde{D}_{st}\,, \widetilde{D}_{ct}]\begin{bmatrix} N_2 \\ I_{d_{RT}-(d_P+p)} \end{bmatrix} = -\widetilde{D}_{ct} + \widetilde{D}_{ct} = 0\,.$$

□

Remark 4. *The functions* $\widetilde{\mathbf{u}}_{h,k}$, $k \in \{1, \dots, d_{RT} - d_P\}$ *form a basis of the space* $RT^0_{h,r+1} = RT_{h,r+1} \cap H^0(\mathrm{div}; \Omega)$. *The first* p *elements* $\widetilde{\mathbf{u}}_{h,k}$, $k \in \{1, \dots, p\}$ *are divergence-free functions that are not the curl of any vector potential. They are representatives of a basis of the second de Rham cohomology group. The remaining* $d_{RT} - (d_P + p)$ *elements* $\widetilde{\mathbf{u}}_{h,p+j}$, $j \in \{1, \dots, d_{RT} - (d_P + p)\}$, *are the curl of vector potentials in the space* $N_{h,r+1}$ *of Nédélec finite elements of degree* $r + 1$, *because they satisfy*

$$\begin{cases} \mathrm{div}\, \widetilde{\mathbf{u}}_{h,p+j} = 0\,, \\ \int_{(\partial\Omega)_l} \widetilde{\mathbf{u}}_{h,p+j} \cdot \mathbf{n}_{\partial\Omega} = 0 \quad \textit{for } l = 1, 2, \dots, p\,. \end{cases}$$

6 Numerical results

In this section we illustrate the performance of the method for the construction of a basis of $RT^0_{h,r+1} := RT_{h,r+1} \cap H^0(\mathrm{div}; \Omega)$ analyzed in Section 5.

The algorithm has been implemented in MATLAB (R2016a). All the numerical computations have been performed by an Intel Core i7-6700HQ, with a processor at 2.60 GHz on a laptop with 12 GB of RAM. The input is a mesh created by TetGen (see [13]), the output is the matrix with the degrees of freedom (moments) of a basis of $RT^0_{h,r+1}$, with a column for each element of the basis, as indicated in Proposition 4.

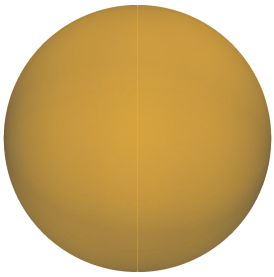

(a) Sphere. $p = 0$.

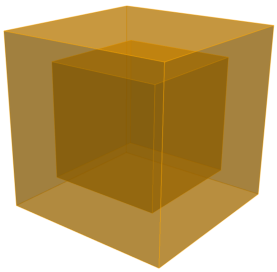

(b) Cube with a cube cavity. $p = 1$.

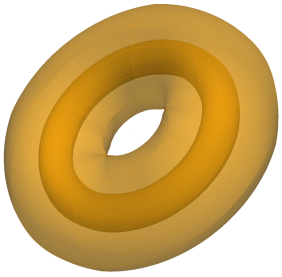

(c) Torus with toroidal cavity. $p = 1$.

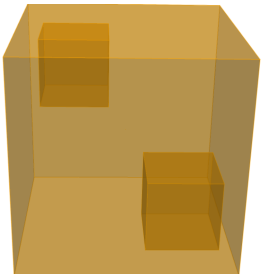

(d) Cube with two cubic cavities. $p = 2$.

Figure 2: The geometry of the considered test cases.

The algorithm has been tested by computing this matrix for $r = 1$ and $r = 2$, in successive uniformly refined meshes of the domains Ω presented in Figure 2. We consider four different test cases. In the first one the domain Ω is a sphere, its boundary is connected, so $p = 0$. In the second test case Ω is a cube with a concentric cubic cavity, the boundary has two connected components, so $p = 1$. In the third test case Ω is a torus with a concentric toroidal cavity, its boundary has two connected components, so $p = 1$. In the last one the domain Ω is a cube with two cubic cavities; the boundary has three connected components, so $p = 2$.

In the tables we report, for each test case, the number of elements of the mesh $n_{\mathcal{T}}$, the dimension d_{RT} of the space $RT_{h,r+1}$, the dimension d_P of the space $P_{h,r}$. In the fourth column, $d_{RT}-d_P$ is the dimension of the space $RT^0_{h,r+1}$. In the fifth column, Prepro. [ms], indicates in milliseconds the time spent to read the mesh, assemble the matrix $\widetilde{D}_{\mathcal{T}_h}$ and build the spanning tree. In the last column, SL [ms], indicates the time in milliseconds spent to solve the $d_{RT}-d_P$ linear systems in equation (9) using the command *backslash* of MATLAB and finally construct the matrix of moments $\widetilde{B} = [\widetilde{B}_1, \widetilde{B}_2] \in \mathbb{R}^{d_{RT}\times(d_{RT}-d_P)}$.

6.1 The case $r = 1$

For the first test case, the sphere, we consider two different spanning trees. In Table 1 (that has in fact seven columns), we report the computational times for eight successive uniformly refined meshes. In the sixth column, SL b.f [ms], we indicate the time in milliseconds for solving the $d_{RT} - d_P$ linear systems in (9) and finally construct the matrix of moments $\widetilde{B} = [\widetilde{B}_1, \widetilde{B}_2] \in \mathbb{R}^{d_{RT}\times(d_{RT}-d_P)}$ when using a spanning tree built by using a breadth-first search. In the last column, SL d.f [ms], we indicate again the time for solving the $d_{RT} - d_P$ linear systems in (9) but now using a spanning tree built by using a depth-first search.

$n_{\mathcal{T}}$	d_{RT}	d_P	$d_{RT} - d_P$	Prepro. [ms]	SL b.f [ms]	SL d.f [ms]
104	1 092	416	676	302.7	0.9	7.8
1 035	10 095	4 140	5 955	384.7	4.1	921.8
2 625	25 488	10 500	14 988	407.0	11.8	6 320.5
7 829	75 078	31 316	43 762	404.8	34.3	103 916.7
15 690	150 516	62 760	87 756	520.4	82.0	-
31 748	299 880	126 992	172 888	791.1	256.7	-
64 239	604 086	256 956	347 130	1 325.0	620.6	-
128 609	1 201 494	514 436	687 058	2 451.5	1 665.7	-

Table 1: Results for the sphere, ($r = 1$).

The results show that the time for solving the $d_{RT} - d_P$ linear systems in (9) is much longer when the spanning tree is built by using a depth-first search. Indeed, the number of elements different from zero in the matrix $\widetilde{B} = [\widetilde{B}_1, \widetilde{B}_2] \in \mathbb{R}^{d_{RT}\times(d_{RT}-d_P)}$,

that contains the moments of a basis of $RT^0_{h,r+1}$, is larger with a depth-first search than that with a breadth-first search spanning tree.

$n_{\mathcal{T}}$	d_{RT}	$d_{RT} - d_P$	Breadth-first [%]	Depth-first [%]
104	1 092	676	0.322	9.06
1 035	10 095	5 955	0.055	7.86
2 625	25 488	14 988	0.024	7.38
7 829	75 078	43 762	0.010	7.51
15 690	50 516	87 756	0.005	-
31 748	299 880	172 888	0.004	-
64 239	604 086	347 130	0.002	-
128 609	1 201 494	687 058	0.001	-

Table 2: Sparsity of the matrix $\widetilde{B}$ containing the moments of a basis of $RT^0_{h,r+1}$, $(r = 1)$.

In Table 2 we report the sparsity of the matrix $\widetilde{B}$ associated to these two kinds of spanning trees.

In Figure 3 we illustrate the behavior, with respect to the dimension of the problem, of the total computational time (on the left), and of the time to solve the $d_{RT} - d_P$ linear systems in (9) (on the right). In the plot on the left, the slope of the curves changes when the considered mesh attains a critical size. Before this critical size, the preprocessing time is more significative than the resolution time, and after, the other way around. This behavior does not depend on the adopted method to construct the spanning tree. In the plot on the right, only the resolution time is considered, which has a rather linear (resp. quadratic) behavior when adopting the breadth-first (resp. depth-first) spanning tree.

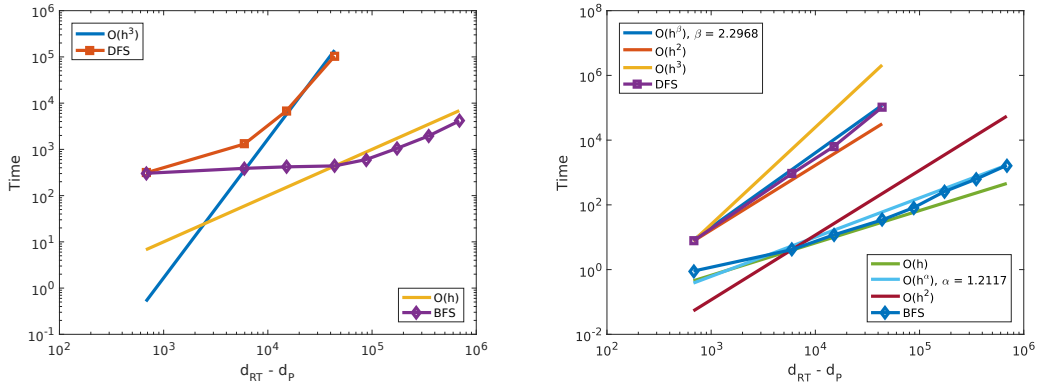

Figure 3: Total computational time (left), and time for solving the linear systems using breadth-first or a depth-first spanning tree (right) in the sphere test case, $(r = 1)$.

For the second, third and fourth test cases, we present numerical results only for a breadth-first spanning tree. These three examples show that the method is successful in

domains with a non connected boundary. In the case of the torus with a toroidal cavity the domain is not simply connected; however this aspect does not influence the performance of the algorithm. The fourth example shows that the algorithm is robust with respect to the number of connected components of the boundary. These considerations are summarized in Figure 4 where we can clearly see that the time for solving the linear systems is independent of the topology of the test case domain and depends only on the dimension of the matrix $\widetilde{D}_{st}$.

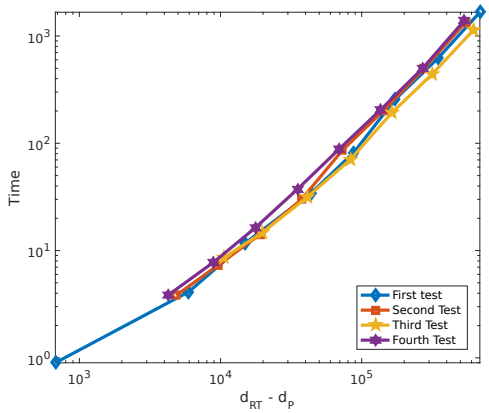

Figure 4: Time for solving the linear systems using breadth-first spanning tree in the four test cases, ($r = 1$).

In Tables 3, 4 and 5, we report the detailed computational times of the second, third and fourth test cases with successive uniformly refined meshes, respectively.

$n_{\mathcal{T}}$	d_{RT}	d_P	$d_{RT} - d_P$	Prepro. [ms]	SL b.f [ms]
807	8 091	3 228	4 863	386.5	3.8
1 606	16 020	6 424	9 596	442.2	7.3
3 221	32 010	12 884	19 126	493.5	14.2
6 468	63 444	25 872	37 572	555.6	30.1
12 964	124 935	51 856	73 079	719.7	86.2
25 940	246 282	103 760	142 522	825.1	201.4
50 995	480 507	203 980	276 527	1 905.4	496.2
102 169	954 693	408 676	546 017	3 896.7	1 346.0

Table 3: Results for the cube with a concentric cubic cavity, ($r = 1$).

Finally, in Figure 5 we plot, on the left, the total computational time, and on the right, the time to solve the $d_{RT} - d_P$ linear systems in (9), both as a function of the problem dimension. We notice again the existence of a critical dimension of the mesh size starting from which the preprocessing time is not longer dominant. In the plot on the right, only the resolution time is considered, which has a rather linear behavior with

$n_{\mathcal{T}}$	d_{RT}	d_P	$d_{RT} - d_P$	Prepro. [ms]	SL b.f [ms]
1 784	17 664	7 136	10 528	424.5	8.5
3 366	33 327	13 464	19 863	487.8	14.8
6 939	68 781	27 756	41 025	648.5	31.4
13 891	138 555	55 564	82 991	655.9	70.4
27 849	274 611	111 396	163 215	998.0	192.2
55 705	540 477	222 820	317 657	1 414.4	444.4
111 345	1 062 786	445 380	617 406	2 576.3	1 133.8

Table 4: Results for the torus with a concentric toroidal cavity, ($r = 1$).

$n_{\mathcal{T}}$	d_{RT}	d_P	$d_{RT} - d_P$	Prepro. [ms]	SL b.f [ms]
719	7 149	2 876	4 273	401.2	3.9
1 530	15 072	6 120	8 952	422.7	7.8
3 098	29 991	12 392	17 599	475.6	16.3
6 280	60 150	25 120	35 030	561.3	37.3
12 577	119 199	50 308	68 891	754.7	87.7
25 293	237 951	101 172	136 779	1 168.0	206.4
50 621	472 260	202 484	269 776	2 556.6	498.8
101 288	937 815	405 152	532 663	3 696.9	1 390.7

Table 5: Results for the cube with two cubic cavities, ($r = 1$).

respect to the problem dimension.

6.2 The case $r = 2$

We use the same meshes as the ones used for the case $r = 1$, and we present tables and figures similar to those of the previous case to show that the algorithm is also robust with respect the polynomial degree r.

$n_{\mathcal{T}}$	d_{RT}	d_P	$d_{RT} - d_P$	Prepro. [ms]	SL b.f [ms]	SL d.f [ms]
104	2 808	1 040	1 768	263.9	0.8	53.6
1 035	26 400	10 350	16 050	359.7	8.7	6 906.5
2 625	66 726	26 250	40 476	398.2	25.9	73 048.1
7 829	197 130	78 290	118 840	550.8	111.6	-
15 690	395 172	156 900	238 272	869.4	285.2	-
31 748	790 248	317 480	472 768	1 518.1	785.2	-
64 239	1 593 606	642 390	951 216	2 990.6	1 819.9	-

Table 6: Results for the sphere, ($r = 2$).

Again, the time for solving the $d_{RT} - d_P$ linear systems in (9) is much longer when using a spanning tree constructed with a depth-first search (see Table 6), since the number of elements different from zero in $\widetilde{B} = [\widetilde{B}_1, \widetilde{B}_2] \in \mathbb{R}^{d_{RT} \times (d_{RT} - d_P)}$ is larger using a depth-first search than that using a breadth-first search spanning tree (see Table 7).

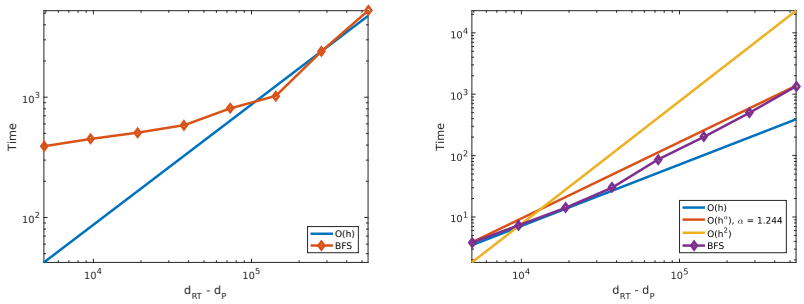

(a) Cube with a cube cavity. $p = 1$.

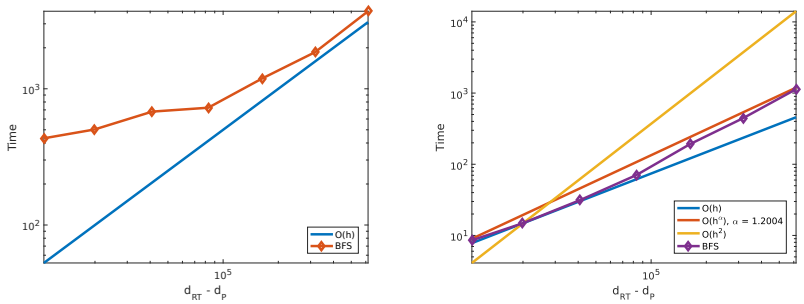

(b) Torus with toroidal cavity. $p = 1$.

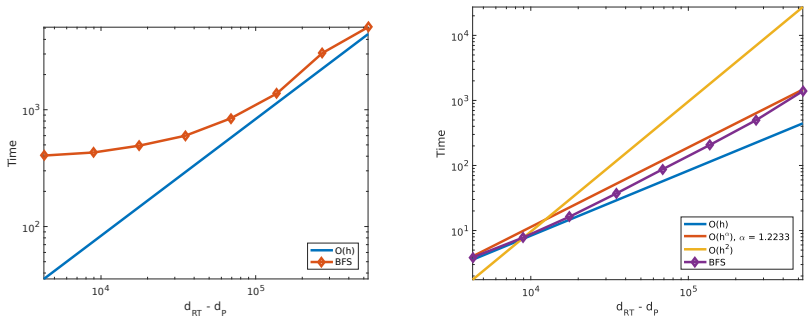

(c) Cube with two cubic cavities. $p = 2$.

Figure 5: Total computational time (left), and time for solving the linear systems (right) in the three test cases with not connected boundary, ($r = 1$).

In Figure 6 we represent the total computational time (on the left), and the time to solve the $d_{RT} - d_P$ linear systems in (9) (on the right), with respect to the dimension of the problem. The behavior of the case $r = 2$ is similar to the behavior of the case $r = 1$, as we can see in Figure 6 and Figure 7.

In Tables 8, 9 and 10, we report the detailed computational times of the second, third and fourth test cases with successive uniformly refined meshes, respectively.

$n_{\mathcal{T}}$	d_{RT}	$d_{RT} - d_P$	Breadth-first [%]	Depth-first [%]
104	2 808	1 768	0.143	8.45
1 035	26 400	16 050	0.024	5.95
2 625	66 726	40 476	0.010	5.51
7 829	197 130	118 840	0.004	-
15 690	395 172	238 272	0.002	-
31 748	790 248	472 768	0.001	-
64 239	1 593 606	951 216	< 0.001	-

Table 7: Sparsity of the matrix $\widetilde{B}$ containing the moments of a basis of $RT^0_{h,r+1}$, $(r = 2)$.

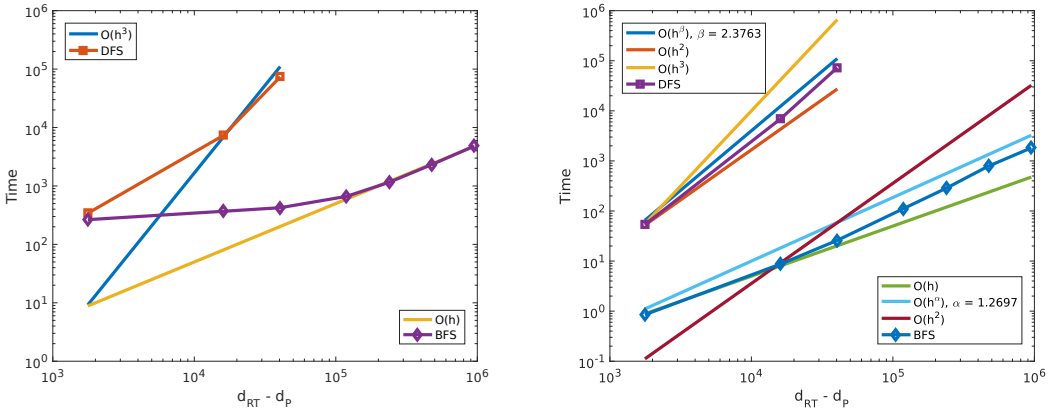

Figure 6: Total computational time (left), and time for solving the linear systems using breadth-first or a depth-first spanning tree (right) in the sphere test case, $(r = 2)$.

Finally, in Figure 8 we plot, on the left, the total computational time, and on the right, the time to solve the $d_{RT} - d_P$ linear systems in (9), both as a function of the problem dimension. We remark again the existence of a critical dimension of the mesh size starting from which the preprocessing time is not longer dominant. In the plot on the right, only the resolution time is considered, which has a rather linear behavior with respect to the problem dimension.

7 Conclusions

We have introduced and analyzed an efficient method for the computation of the moments of a function in the space of Raviart-Thomas finite elements of degree $r + 1$ with assigned divergence. The proposed algorithm is based on basic results from graph theory. It turns to be so performant that it can be used to construct a basis of the space RT^0_h of divergence-free Raviart-Thomas elements of any degree.

Concerning the construction of a basis of divergence-free Raviart-Thomas finite ele-

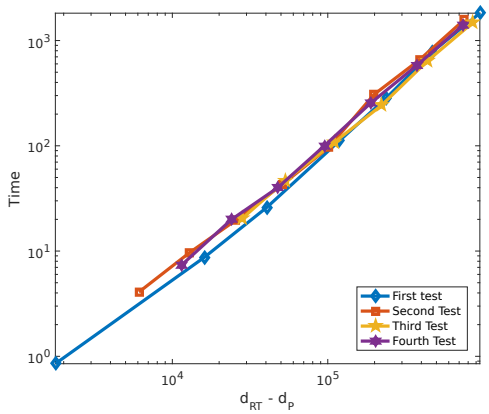

Figure 7: Time for solving the linear systems using breadth-first spanning tree in the four test cases, $(r = 2)$.

$n_{\mathcal{T}}$	d_{RT}	d_P	$d_{RT} - d_P$	Prepro. [ms]	SL b.f [ms]
807	9 936	3 840	6 096	300.3	4.1
1 606	21 024	8 070	12 954	417.5	9.7
3 221	41 676	16 060	25 616	429.1	19.7
6 468	83 346	32 210	51 136	511.6	43.0
12 964	165 696	64 680	101 016	658.4	96.2
25 940	327 654	129 640	198 014	965.9	306.5
50 995	648 204	259 400	388 804	1 646.2	655.4
102 169	1 266 984	509 950	757 034	3 071.5	1 582.1

Table 8: Results for the cube with a concentric cubic cavity, $(r = 2)$.

ments of degree $r+1$, for $r = 1$ and $r = 2$, the numerical tests show that the efficiency of the algorithm is analogous in the two cases and that the behavior depends on the dimension of the finite elements space but not on the degree of the approximation. Moreover, it is robust with respect to the topology of the domain. When using a breadth-first spanning tree on big enough meshes, the computational time is of order ≈ 1.2 with respect to the dimension $d_{RT} - d_P$ of RT_h^0.

Acknowledgment

The second author was partially supported by CONICYT-Chile through Fondecyt project 1180859 and the project AFB170001 of the PIA Program: Concurso Apoyo a Centros Cientificos y Tecnologicos de Excelencia con Financiamiento Basal. The third author was partially supported by a CONICYT (Chile) fellowship.

$n_{\mathcal{T}}$	d_{RT}	d_P	$d_{RT} - d_P$	Prepro. [ms]	SL b.f [ms]
1 784	46 032	17 840	28 192	427.1	20.4
3 366	86 850	33 660	53 190	484.1	46.6
6 939	179 196	69 390	109 806	765.2	107.2
13 891	360 456	138 910	221 546	889.5	242.2
27 849	716 316	278 490	437 826	1 581.9	640.2
55 705	1 415 184	557 050	858 134	2 792.3	1 482.4

Table 9: Results for the torus with a concentric toroidal cavity, ($r = 2$).

$n_{\mathcal{T}}$	d_{RT}	d_P	$d_{RT} - d_P$	Prepro. [ms]	SL b.f [ms]
719	18 612	7 190	11 422	372.9	7.3
1 530	39 324	15 300	24 024	411.6	19.9
3 098	78 570	30 980	47 590	476.3	39.9
6 280	157 980	62 800	95 180	635.0	100.1
12 577	313 860	125 770	188 090	998.5	253.4
25 293	627 660	252 930	374 730	1 702.7	581.8
50 621	1 248 246	506 210	742 036	3 069.8	1 401.8

Table 10: Results for the cube with two cubic cavities, ($r = 2$).

References

[1] A. Alonso Rodríguez, E. Bertolazzi, and A. Valli, *Simple finite element schemes for the solution of the curl-div system.* arXiv:1512.08532v1, 2015.

[2] A. Alonso Rodríguez, J. Camaño, R. Ghiloni, and A. Valli, *Graphs, spanning trees and divergence-free finite elements in domains of general topology*, IMA J. Numer. Anal., 37 (2017), pp. 1986–2003.

[3] A. Alonso Rodríguez and A. Valli, *Finite element potentials*, Appl. Numer. Math., 95 (2015), pp. 2–14.

[4] P. Alotto and I. Perugia, *Mixed finite element methods and tree-cotree implicit condensation*, Calcolo, 36 (1999), pp. 233–248.

[5] M. Bonazzoli and F. Rapetti, *High-order finite elements in numerical electromagnetism: degrees of freedom and generators in duality*, Numer. Algorithms, 74 (2017), pp. 111–136.

[6] W. Cai, J. Wu, and J. Xin, *Divergence-free $\mathcal{H}(\mathrm{div})$-conforming hierarchical bases for magnetohydrodynamics (MHD)*, Commun. Math. Stat., 1 (2013), pp. 19–35.

[7] Z. Cai, R. R. Parashkevov, T. F. Russell, J. D. Wilson, and X. Ye, *Domain decomposition for a mixed finite element method in three dimensions*, SIAM J. Numer. Anal., 41 (2003), pp. 181–194.

[8] J. Cantarella, D. DeTurck, and H. Gluck, *Vector calculus and the topology of domains in 3-space*, Amer. Math. Monthly, 109 (2002), pp. 409–442.

[9] F. Dubois, *Discrete vector potential representation of a divergence-free vector field in three-dimensional domains: numerical analysis of a model problem*, SIAM J. Numer. Anal., 27 (1990), pp. 1103–1141.

[10] D. F. Griffiths, *An approximately divergence-free* 9*-node velocity element (with variations) for incompressible flows*, Internat. J. Numer. Methods Fluids, 1 (1981), pp. 323–346.

[11] K. Gustafson and R. a. Hartman, *Divergence-free bases for finite element schemes in hydrodynamics*, SIAM J. Numer. Anal., 20 (1983), pp. 697–721.

[12] C. A. Hall and X. Ye, *Construction of null bases for the divergence operator associated with incompressible Navier-Stokes equations*, Linear Algebra Appl., 171 (1992), pp. 9–52.

[13] F. Hecht, *Construction d'une base de fonctions* P_1 *non conforme à divergence nulle dans* $\mathbf{R}^3$, RAIRO Anal. Numér., 15 (1981), pp. 119–150.

[14] S. Le Borne and D. Cook, II, *Construction of a discrete divergence-free basis through orthogonal factorization in* $\mathcal{H}$*-arithmetic*, Computing, 81 (2007), pp. 215–238.

[15] P. Monk, *Finite element methods for Maxwell's equations*, Numerical Mathematics and Scientific Computation, Oxford University Press, New York, 2003.

[16] J.-C. Nédélec, *Mixed finite elements in* $\mathbf{R}^3$, Numer. Math., 35 (1980), pp. 315–341.

[17] F. Rapetti, F. Dubois, and A. Bossavit, *Discrete vector potentials for non-simply connected three-dimensional domains*, SIAM J. Numer. Anal., 41 (2003), pp. 1505–1527.

[18] P.-A. Raviart and J.-M. Thomas, *A mixed finite element method for 2nd order elliptic problems*, in Mathematical aspects of finite element methods (Proc. Conf., Consiglio Naz. delle Ricerche Rome, 1975), vol. 606 of Lecture Notes in Mathematics, 1977, pp. 292–315.

[19] R. Scheichl, *Decoupling three-dimensional mixed problems using divergence-free finite elements*, SIAM J. Sci. Comput., 23 (2002), pp. 1752–1776.

[20] K. Thulasiraman and M. Swamy, *Graphs: theory and algorithms*, A Wiley-Interscience Publication, John Wiley & Sons, Inc., New York, 1992.

[21] J. Wang, Y. Wang, and X. Ye, *A robust numerical method for Stokes equations based on divergence-free $H(\mathrm{div})$ finite element methods*, SIAM J. Sci. Comput., 31 (2009), pp. 2784–2802.

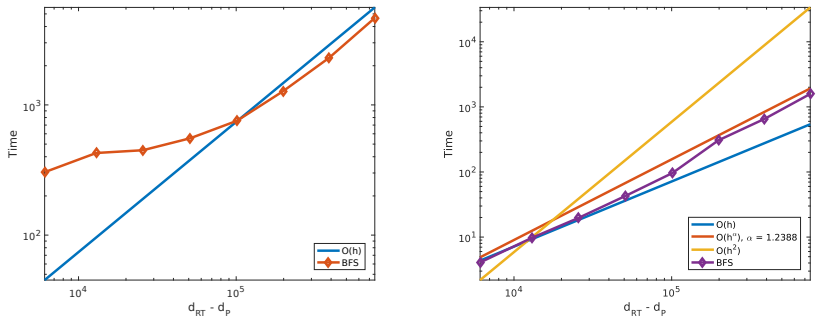

(a) Cube with a cube cavity. $p = 1$.

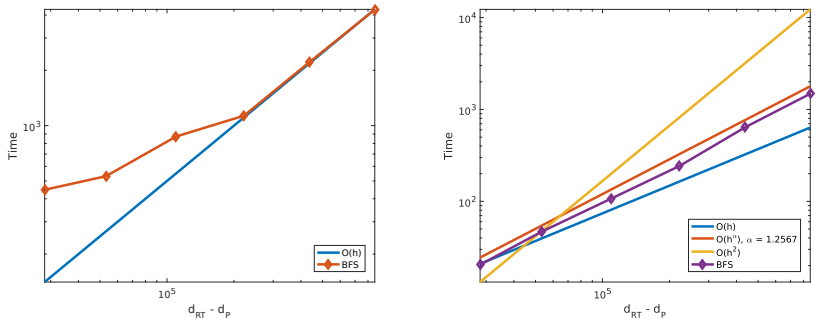

(b) Torus with toroidal cavity. $p = 1$.

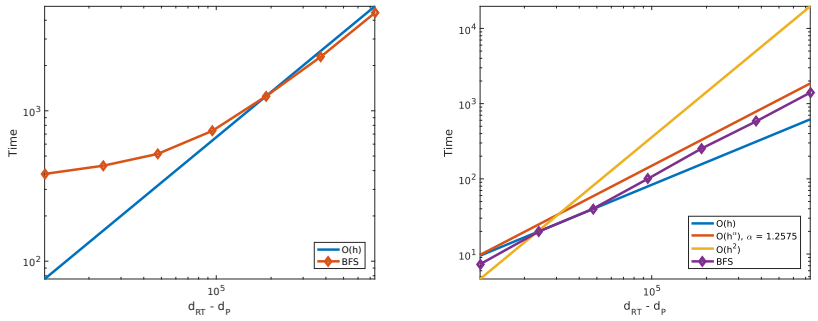

(c) Cube with two cubic cavities. $p = 2$.

Figure 8: Total computational time (left), and time for solving the linear systems (right) in the three test cases with not connected boundary, ($r = 2$).

Centro de Investigación en Ingeniería Matemática (CI^{2}MA)

PRE-PUBLICACIONES 2018

2018-12 Alfredo Bermúdez, Bibiana López-Rodríguez, Rodolfo Rodríguez, Pilar Salgado: *Numerical solution of a transient three-dimensional eddy current model with moving conductors*

2018-13 Raimund Bürger, Enrique D. Fernández Nieto, Victor Osores: *A dynamic multilayer shallow water model for polydisperse sedimentation*

2018-14 Antonio Baeza, Raimund Bürger, Pep Mulet, David Zorío: *Weno reconstructions of unconditionally optimal high order*

2018-15 Veronica Anaya, Mostafa Bendahmane, David Mora, Mauricio Sepúlveda: *A virtual element method for a nonlocal FitzHugh-Nagumo model of cardiac electrophysiology*

2018-16 Tomás Barrios, Rommel Bustinza: *An a priori error analysis for discontinuous Lagrangian finite elements applied to nonconforming dual mixed formulations: Poisson and Stokes problems*

2018-17 Raimund Bürger, Gerardo Chowell, Elvis Gavilán, Pep Mulet, Luis M. Villada: *Numerical solution of a spatio-temporal predator-prey model with infected prey*

2018-18 Javier A. Almonacid, Gabriel N. Gatica, Ricardo Oyarzúa, Ricardo Ruiz-Baier: *A new mixed finite element method for the n-dimensional Boussinesq problem with temperature-dependent viscosity*

2018-19 Antonio Baeza, Raimund Bürger, María Carmen Martí, Pep Mulet, David Zorío: *Approximate implicit Taylor methods for ODEs*

2018-20 Raimund Bürger, Daniel Inzunza, Pep Mulet, Luis M. Villada: *Implicit-explicit schemes for nonlinear nonlocal equations with a gradient flow structure in one space dimension*

2018-21 Ricardo Oyarzúa, Miguel Serón: *A divergence-conforming DG-mixed finite element method for the stationary Boussinesq problem*

2018-22 Veronica Anaya, Afaf Bouharguane, David Mora, Carlos Reales, Ricardo Ruiz-Baier, Nour Seloula, Hector Torres: *Analysis and approximation of a vorticity-velocity-pressure formulation for the Oseen equations*

2018-23 Ana Alonso-Rodriguez, Jessika Camaño, Eduardo De Los Santos, Francesca Rapetti: *A graph approach for the construction of high order divergence-free Raviart-Thomas finite elements*

Para obtener copias de las Pre-Publicaciones, escribir o llamar a: Director, Centro de Investigación en Ingeniería Matemática, Universidad de Concepción, Casilla 160-C, Concepción, Chile, Tel.: 41-2661324, o bien, visitar la página web del centro: `http://www.ci2ma.udec.cl`







Centro de Investigación en
Ingeniería Matemática (CI²MA)
Universidad de Concepción

Casilla 160-C, Concepción, Chile
Tel.: 56-41-2661324/2661554/2661316
http://www.ci2ma.udec.cl